Differential Geometry and its Applications 30 (2012) 405–427

Contents lists available at SciVerse ScienceDirect

Differential Geometry and its Applications

www.elsevier.com/locate/difgeo

# A Monster Tower approach to Goursat multi-flags

Alex L. Castro [a,1], Wyatt C. Howard [b,*]

[a] Departamento de Matemática, Pontifícia Universidade Católica do Rio de Janeiro, Brazil
[b] Mathematics Department, University of California at Santa Cruz, United States

ARTICLE INFO

*Article history:*
Received 23 July 2011
Received in revised form 12 April 2012
Available online 2 July 2012
Communicated by M.G. Eastwood

*MSC:*
primary 58A30
secondary 58A17, 58K50

*Keywords:*
Goursat multi-flags
Prolongation
Semple tower

ABSTRACT

We consider the problem of classifying the orbits within a tower of fibrations with $\mathbb{P}^2$-fibers that generalize the Monster Tower due to Montgomery and Zhitomirskii. The action on the tower is given by prolongations of diffeomorphism germs of 3-space. As a corollary we give the first steps towards the problem of classifying Goursat 2-flags of small length. In short, we classify the orbits within the first four levels of the Monster Tower and show that there is a total of 34 orbits in the fourth level of the tower.



## 1. Introduction

A Goursat flag is a nonholonomic distribution $D$ with *slow growth*. By slow growth we mean that the rank of the associated flag of distributions

$$D \quad \subset \quad D + [D, D] \quad \subset \quad D + [D, D] + \big[[D, D], [D, D]\big] \ldots$$

grows by one at each bracketing step. The condition of nonholonomy guarantees that after sufficiently many steps we will obtain the entire tangent bundle of the ambient manifold. By an abuse of notation, $D$ in this context also denotes the sheaf of vector fields spanning $D$.

Though less popular than her other nonholonomic siblings like the contact distribution, or rolling distribution in mechanics [4], Goursat distributions are more common than one would think. The canonical Cartan distributions in the jet spaces $J^k(\mathbb{R}, \mathbb{R})$ and the non-slip constraint for a jackknifed truck [9] are examples.

Generalizations of Goursat flags have been proposed in the literature. One such notion is that of a *Goursat multi-flag*. A Goursat $n$-flag of length $k$ is a distribution of rank $(n+1)$ sitting in an $(n+1)+kn$ dimensional ambient manifold, where the rank of the associated flag increases by $n$ at each bracketing step. For clarity, we have included the exact definition in Appendix A to the paper. A well-known example of a Goursat multi-flag is the Cartan distribution $C$ of the jet spaces $J^k(\mathbb{R}, \mathbb{R}^n)$. Iterated bracketing this time produces a flag of distributions

$$C \quad \subset \quad C + [C, C] \quad \subset \quad C + [C, C] + \big[[C, C], [C, C]\big] \ldots,$$

where the rank jumps by $n$ at each step.

* Corresponding author.
*E-mail addresses:* alex.castro@mat.puc-rio.br (A.L. Castro), whoward@ucsc.edu (W.C. Howard).
[1] Tel.: +55 21 3527 1722.

0926-2245/$ – see front matter 
http://dx.doi.org/10.1016/j.difgeo.2012.06.005

To our knowledge the general theory behind Goursat multi-flags made their first appearance in the works of A. Kumpera and J.L. Rubin [11]. P. Mormul has also been very active in breaking new ground [15], and developed new combinatorial tools to investigate the normal forms of these distributions. Our work is founded on a recent article [22] by Shibuya and Yamaguchi that demonstrates a universality result which essentially states that any Goursat multi-flag arises as a type of lifting of the tangent bundle of $\mathbb{R}^n$.

In this paper we concentrate on the problem of classifying Goursat multi-flags of small length. Specifically, we will consider Goursat 2-flags of length up to 4. Goursat 2-flags exhibit many new geometric features our old Goursat 1-flags did not possess [19].

*Our main result states that there are* 34 *inequivalent Goursat* 2*-flags of length* 4 *and we provide the exact number of Goursat* 2*-flags for each length* $k \leqslant 3$ *as well.*

Our approach is constructive. Due to space limitations we will write down only a few instructive examples.

In [22] Shibuya and Yamaguchi establish that every Goursat 2-flag germ appears somewhere within the following tower of fiber bundles:

$$\cdots \to \mathcal{P}^4(2) \to \mathcal{P}^3(2) \to \mathcal{P}^2(2) \to \mathcal{P}^1(2) \to \mathcal{P}^0(2) = \mathbb{R}^3, \tag{1}$$

and the fiber of the projection map from $\mathcal{P}^k(2)$ to $\mathcal{P}^{k-1}(2)$ is a real projective plane, and adding the dimensions one obtains the dimension formula $\dim(\mathcal{P}^k(2)) = 3 + 2k$.

Each manifold $\mathcal{P}^k(2)$ is equipped with a rank 3 nonholonomic distribution $\Delta_k$, and there is a simple geometric relation between the distributions pertaining to neighboring levels. The construction of $\Delta_k$ is recursive, and depends upon the geometric data at the base level $\mathcal{P}^0$.

The distributions $\Delta_k$ in $\mathcal{P}^k(2)$ are themselves Goursat 2-flags of length $k$. Moreover, two Goursat 2-flags are equivalent if and only if the corresponding points of the Monster Tower are mapped one to the other by a *symmetry* of the tower at level $k$. The paper [22] also establishes that all such symmetries are prolongations of diffeomorphisms of $\mathbb{R}^3$. The above observations tell us that

*the classification problem for Goursat* 2*-flags is equivalent to the classification of points within the Monster Tower up to symmetry.*

In order to solve this latter problem we use a combination of two methods, namely the singular curve method as in [18] and a new method that we call the *isotropy method*. A variant of the isotropy method was already used in [18], and it is somewhat inspired by É. Cartan's *moving frame* method [8].

We would like to mention that P. Mormul and Pelletier [17] have proposed an alternative solution to the classification problem. In their classification work, they employed Mormul's results and tools that came from his recent work with Goursat $n$-flags. In [16], Mormul discusses two coding systems for special 2-flags and showed that the two coding systems are the same. One system is the *extended Kumpera–Ruiz system*, which is a coding system used to describe 2-flags. The other is called *singularity class coding*, which is an intrinsic coding system that describes the sandwich diagram [18] associated to 2-flags. A brief outline on how these coding systems relate to the $RVT$ coding is discussed in [6]. Then, building upon Mormul's work in [14], Mormul and Pelletier used the idea of strong nilpotency of special multi-flags, along with the properties of his two coding systems, to classify these distributions up to length 4. Our 34 orbits agree with theirs.

In Section 2 we acquaint ourselves with the main definitions necessary for the statements of our main results, and a few explanatory remarks to help the reader progress through the theory with us. Section 3 consists of the statements of our main results. In Section 4 we discuss the basic tools and ideas that will be needed to prove our various results. Section 5 is devoted to technicalities and the actual proofs. Finally, in Section 6, we provide a quick summary of our findings and other questions to pursue concerning the Monster Tower.

For the record, we have also included Appendix A where our lengthy computations are contained.

## 2. Preliminaries and main definitions

A *geometric distribution* hereafter denotes a linear subbundle of the tangent bundle with fibers of constant dimension.

### 2.1. Prolongation

Let the pair $(Z, \Delta)$ denote a manifold $Z$ of dimension $d$ equipped with a distribution $\Delta$ of rank $r$. We denote by $\mathbb{P}(\Delta)$ the *projectivization* of $\Delta$. As a manifold,

$$\mathbb{P}(\Delta) \equiv Z^1$$

has dimension $d + (r - 1)$.

**Example 2.1.** Take $Z = \mathbb{R}^3$, $\Delta = TR^3$ viewed as a rank 3 distribution. Then $Z^1$ is simply the trivial bundle $\mathbb{R}^3 \times \mathbb{P}^2$, where the factor on the right denotes the projetive plane.

**Table 1**
Some geometric objects and their Cartan prolongations.

| | |
|---|---|
| curve $c : (I, 0) \to (Z, q)$ | curve $c^1 : (I, 0) \to (Z^1, q)$, $c^1(t) = (\text{point, moving line}) = (c(t), span\{\frac{dc}{dt}(t)\})$ |
| diffeomorphism $\Phi : Z \circlearrowleft$ | diffeomorphism $\Phi^1 : Z^1 \circlearrowleft$, $\Phi^1(p, \ell) = (\Phi(p), d\Phi_p(\ell))$ |
| rank $r$ linear subbundle $\Delta \subset TZ$ | rank $r$ linear subbundle $\Delta_{1(p,\ell)} = d\pi^{-1}_{(p,\ell)}(\ell) \subset TZ^1$, $\pi : Z^1 \to Z$ is the canonical projection. |

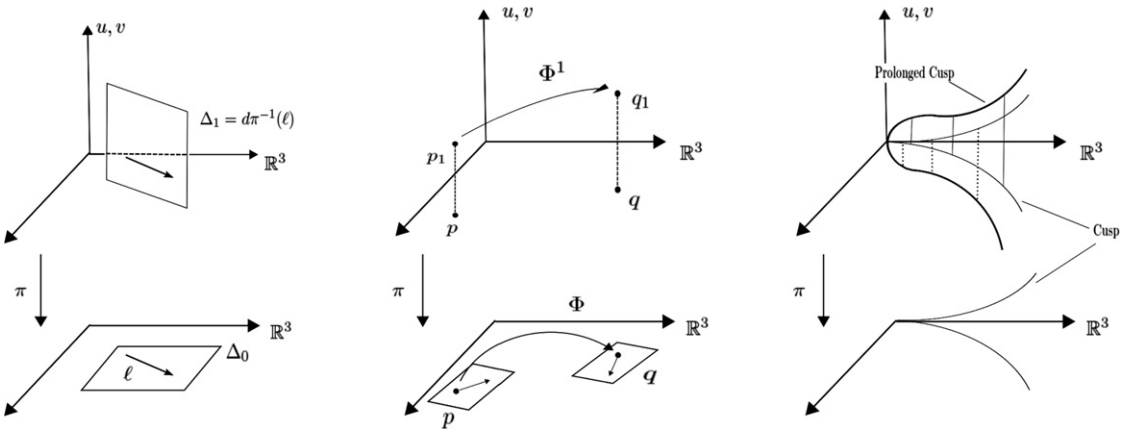


(A) Prolongation of a distribution

(B) Prolongation of a diffeomorphism

(C) Prolongation of a curve

**Fig. 1.** Prolongations.

Various geometric objects in $Z$ can be canonically prolonged (lifted) to the new manifold $Z^1$. In what follows prolongations of curves and transformations are quintessential.

Given an analytic curve $c : (I, 0) \to (Z, q)$, where $I$ is some open interval in $\mathbb{R}$ containing the origin and $c(0) = q$, we can naturally define a new curve

$$c^1 : (I, 0) \to \big(Z^1, (q, \ell)\big)$$

with image in $Z^1$ and where $\ell = span\{\frac{dc}{dt}(0)\}$. This new curve, $c^1(t)$, is called the *prolongation* of $c(t)$. If $t = t_0$ is not a regular point, then we define $c^1(t_0)$ to be the limit $\lim_{t\to t_0} c^1(t)$ where the limit varies over the regular points $t \to t_0$. An important fact to note, proved in [18], is that the analyticity of $Z$ and $c$ implies that the limit is well defined and that the prolonged curve $c^1(t)$ is analytic as well. Since this process can be iterated, we will write $c^k(t)$ to denote the $k$-fold prolongation of the curve $c(t)$.

The manifold $Z^1$ also comes equipped with a distribution $\Delta_1$ called the *Cartan prolongation of* $\Delta$ [3] which is defined as follows. Let $\pi : Z^1 \to Z$ be the projection map $(p, \ell) \mapsto p$. Then

$$\Delta_1(p, \ell) = d\pi^{-1}_{(p,\ell)}(\ell),$$

i.e. *it is the subspace of* $T_{(p,\ell)}Z^1$ *consisting of all tangents to curves which are prolongations of curves in* $Z$ *that pass through* $p$ *with a velocity vector contained in* $\ell$. It is easy to check using linear algebra that $\Delta_1$ is also a distribution of rank $r$.

By a *symmetry* of the pair $(Z, \Delta)$ we mean a local diffeomorphism $\Phi$ of $Z$ that preserves the subbundle $\Delta$.

The symmetries of $(Z, \Delta)$ can also be prolonged to symmetries $\Phi^1$ of $(Z^1, \Delta_1)$ as follows. Define

$$\Phi^1(p, \ell) := \big(\Phi(p), d\Phi_p(\ell)\big).$$

Since[2] $d\Phi_p$ is invertible and $d\Phi_p$ is linear the second component is well defined as a projective map. This new transformation in $(Z^1, \Delta_1)$ is the *prolongation* of $\Phi$. Objects of interest and their Cartan prolongations are summarized in Table 1. We note that the word prolongation will always be synonymous with Cartan prolongation (see Fig. 1).

[2] We also use the notation $\Phi_*$ for the pushforward or tangent map $d\Phi$.

**Example 2.2** *(Prolongation of a cusp).* Let $c(t) = (t^2, t^3, 0)$ be the cusp or semi-cubical parabola viewed as a curve in $\mathbb{R}^3$. Then $c^1(t) = (x(t), y(t), z(t), [dx : dy : dz]) = (t^2, t^3, 0, [2t : 3t^2 : 0])$. After we introduce fiber affine coordinates $u = \frac{dy}{dx}$ and $v = \frac{dz}{dx}$ around the point $(0, 0, 0, [1 : 0 : 0])$ we obtain the immersed curve

$$c^1(t) = \left(t^2, t^3, 0, \frac{3}{2}t, 0\right).$$

### 2.2. Constructing the Monster Tower

We start with $\mathbb{R}^{n+1}$ as our base manifold $Z$ and take $\Delta_0 = T\mathbb{R}^{n+1}$. Prolonging $\Delta_0$ we get $\mathcal{P}^1(n) = \mathbb{P}(\Delta_0)$ equipped with the distribution $\Delta_1$ of rank $n$. By iterating this process we end up with the manifold $\mathcal{P}^k(n)$ which is endowed with the rank $n$ distribution $\Delta_k = (\Delta_{k-1})^1$ and fibered over $\mathcal{P}^{k-1}(n)$. In this paper we will be studying the case $n = 2$.

**Definition 2.1.** The *Monster Tower* is a sequence of manifolds with distributions, $(\mathcal{P}^k, \Delta_k)$, together with fibrations

$$\cdots \to \mathcal{P}^k(n) \to \mathcal{P}^{k-1}(n) \to \cdots \to \mathcal{P}^1(n) \to \mathcal{P}^0(n) = \mathbb{R}^{n+1}$$

and we write $\pi_{k,i} : \mathcal{P}^k(n) \to \mathcal{P}^i(n)$ for the respective bundle projections.

This explains how the tower shown in Eq. (1) is obtained by iterated Cartan prolongation of the pair $(\mathbb{R}^3, \Delta_0)$.

**Definition 2.2.** *Diff*(3) is taken to be the *pseudogroup of diffeomorphism germs of* $\mathbb{R}^3$.

**Remark 2.3** *(The pseudogroup Diff*(3)*).* Saying that *Diff*(3) is a *pseudogroup* roughly means that for any open set $U \subseteq \mathbb{R}^3$, the identity restricted to this set is an element of *Diff*(3), and for any local diffeomorphism in *Diff*(3) defined on $U$ its inverse, defined on $\Phi(U)$ is in *Diff*(3) as well. Also, for any $\Phi_1, \Phi_2 \in$ *Diff*(3) where $\Phi_1 : U_1 \to V_1$ and $\Phi_2 : U_2 \to V_2$, for $U_i$ and $V_i$ open subsets of $\mathbb{R}^3$ with $V_1 \cap U_2 \neq \emptyset$, then the composition $\Phi_2 \circ \Phi_1^{-1} : \Phi_1^{-1}(V_1 \cap U_2) \to \Phi_2(V_1 \cap U_2)$ is an element of *Diff*(3). A more detailed discussion about pseudogroups can be found in [10].

The following result found in a recent paper by Shibuya and Yamaguchi will be important for our classification of points within the Monster Tower.

**Theorem 2.4.** *For $n > 1$ and $k > 0$ any local diffeomorphism of $\mathcal{P}^k(n)$ preserving the distribution $\Delta_k$ is the restriction of the $k$-th prolongation of a local diffeomorphism $\Phi \in$ Diff$(n)$.*

**Proof.** See [22, p. 795]. □

Shibuya and Yamaguchi also point out that this is a result due to A. Bäcklund [2].

**Remark 2.5.** The importance of the above result cannot be stressed enough. This theorem is the theoretical foundation for the isotropy method, discussed in Section 5 of the paper. It will be crucial for classifying orbits within the Monster Tower.

**Remark 2.6.** Since we will be working exclusively with the $n = 2$ Monster Tower in this paper, we will just write $\mathcal{P}^k$ for $\mathcal{P}^k(2)$.

**Definition 2.3.** Two points $p, q$ in $\mathcal{P}^k$ are said to be *equivalent*, written $p \sim q$, if there is a $\Phi \in$ *Diff*(3) such that $\Phi^k(p) = q$.

**Definition 2.4.** Let $p \in \mathcal{P}^k$ then we denote $\mathcal{O}(p)$ to be the *orbit of the point* $p$ under the action by elements of *Diff*(3) to the $k$-th level of the Monster Tower, where a point $q$ is an element in $\mathcal{O}(p)$ if $q$ is equivalent to the point $p$.

### 2.3. Orbits

Theorem 2.4 tells us that any symmetry of $\mathcal{P}^k$ comes from prolonging a diffeomorphism of a real affine three-space $k$ times. Let us denote by $\mathcal{O}(p)$ the orbit of the point $p$ under the action of *Diff*(3).

In trying to calculate the various orbits within the Monster Tower we found it convenient to fix the base points from which they originated from in $\mathbb{R}^3$. In particular, if $p_k$ is a point in $\mathcal{P}^k$ and $p_0 = \pi_{k,0}(p_k)$ is the base point in $\mathbb{R}^3$, then by a change of coordinates we can take the point $p_0$ to be the origin in $\mathbb{R}^3$. This means that we can replace the pseudogroup *Diff*(3), diffeomorphism germs of $\mathbb{R}^3$, by the group $Diff_0(3)$ of diffeomorphism germs that map the origin back to the origin in $\mathbb{R}^3$.

**Table 2**
Number of orbits within the first three levels of the Monster Tower.

| Level of tower | $RVT$ code | Number of orbits | Normal forms |
|---|---|---|---|
| 1 | $R$ | 1 | $(t,0,0)$ |
| 2 | $RR$ | 1 | $(t,0,0)$ |
| | $RV$ | 1 | $(t^2,t^3,0)$ |
| 3 | $RRR$ | 1 | $(t,0,0)$ |
| | $RRV$ | 1 | $(t^2,t^5,0)$ |
| | $RVR$ | 1 | $(t^2,t^3,0)$ |
| | $RVV$ | 1 | $(t^3,t^5,t^7)$, $(t^3,t^5,0)$ |
| | $RVT$ | 2 | $(t^3,t^4,t^5)$, $(t^3,t^4,0)$ |
| | $RVL$ | 1 | $(t^4,t^6,t^7)$ |

**Definition 2.5.** We say that a curve or curve germ $\gamma:(\mathbb{R},0)\to(\mathbb{R}^3,\mathbf{0})$ *realizes* the point $p_k\in\mathcal{P}^k$ if $\gamma^k(0)=p_k$, where $p_0=\pi_{k,0}(p_k)\equiv\mathbf{0}$.

It is important to note at this point that prolongation and projection commute. This fact is discussed in detail in [19] and in [6].

**Definition 2.6.** A direction $\ell\subset\Delta_k(p_k)$, $k\geqslant 1$, is called a *critical direction* if there exists an immersed curve at level $k$ that is tangent to the direction $\ell$, and whose projection to level zero, meaning the base manifold, is a constant curve. If no such curve exists, then we call $\ell$ a *regular direction*. Note that while $\ell$ is technically a line we will by an abuse of terminology refer to it as a direction.

**Definition 2.7.** Let $p\in\mathcal{P}^k$. The set of curves

$$Germ(p):=\left\{c:(\mathbb{R},0)\to\left(\mathbb{R}^3,\mathbf{0}\right)\;\middle|\;c^k(0)=p \text{ and } \left.\frac{dc^k}{dt}\right|_{t=0}\neq 0 \text{ is a regular direction}\right\}$$

is called the *germ associated to the point* $p$.

**Definition 2.8.** Two curves $\gamma$, $\sigma$ in $\mathbb{R}^3$ are *RL equivalent*, written $\gamma\sim\sigma$ if there exist a diffeomorphism germ $\Phi\in Diff(3)$ and a reparametrization $\tau\in Diff_0(1)$ such that $\sigma=\Phi\circ\gamma\circ\tau$.

We can then define $Germ(p)\sim Germ(q)$ to mean that every curve in $Germ(p)$ is $RL$ equivalent to some curve in $Germ(q)$ and conversely, every curve in $Germ(q)$ is $RL$ equivalent to some curve in $Germ(p)$.

## 3. Main results

**Theorem 3.1** *(Orbit counting per level). In the* $n=2$ *(or spatial) Monster Tower the number of orbits within each of the first four levels of the tower are as follows*:

- *Level* 1 *has* 1 *orbit.*
- *Level* 2 *has* 2 *orbits.*
- *Level* 3 *has* 7 *orbits.*
- *Level* 4 *has* 34 *orbits.*

The main idea behind determining the number of orbits in the first four levels of the tower is to use a blend of the singular curve methods as introduced in [19] and a technique we call the isotropy method (adapted from [18]). The curve method alone suffices to yield Theorem 3.1 up to level 3. In order to get to level 4 we must use the isotropy method in combination with a classification of special directions which generalizes the $RVT$ coding of [19]. This classification, or *coding* is described in Section 4.3. Our main result, in detail, is the following theorem, of which Theorem 3.1 is an immediate corollary.

**Theorem 3.2** *(Listing of orbits within each* $RVT$ *code). Table 2 is a breakdown of the number of orbits that appear within each* $RVT$ *class within the first three levels.*

*For level* 4 *there is a total of* 23 *possible* $RVT$ *classes. Of the* 23 *possibilities* 14 *of them consist of a single orbit. The classes* $RRVT$, $RVRV$, $RVVR$, $RVVV$, $RVVT$, $RVTR$, $RVTV$, $RVTL$ *consist of* 2 *orbits, and the class* $RVTT$ *consists of* 4 *orbits.*

**Remark 3.3.** There are a few words that should be said to explain the normal forms column in Table 2. Let $p_k\in\mathcal{P}^k$, for $k=1,2,3$, have $RVT$ code $\omega$, meaning $\omega$ is a word from the second column of the table. Let $\gamma\in Germ(p_k)$, then $\gamma$ is $RL$ equivalent to one of the curves listed in the normal forms column for the $RVT$ class $\omega$. Now, for the class $RVV$ we notice

that there are two inequivalent curves sitting in the normal forms column, but that there is only one orbit within that class. This is because the two normal forms are equal to each other, at $t = 0$, after three prolongations. However, after four prolongations they represent different points at the fourth level. This corresponds to the fact that at the fourth level class $RVVR$ breaks up into two orbits.

The following theorems are in [6] and helped to reduce the number calculations in our orbit classification process.

**Definition 3.1.** A point $p_k \in \mathcal{P}^k$ is called a *Cartan point* if its $RVT$ code is $R^k$, where $R^k = \underbrace{R \cdots R}_{k \text{ times}}$.

**Theorem 3.4.** *The $RVT$ class $R^k$ forms a single orbit at any level within the Monster Tower $\mathcal{P}^k(n)$ for $k \geqslant 1$ and $n \geqslant 1$. Every point at level 1 is a Cartan point. For $k > 1$ the set $R^k$ is an open dense subset of $\mathcal{P}^k(n)$.*

**Definition 3.2.** A parametrized curve belongs to the $A_{2k}$ class, $k \geqslant 1$, if it is $RL$ equivalent to the curve

$$\left(t^2, t^{2k+1}, 0\right).$$

**Theorem 3.5.** *Let $p_k \in \mathcal{P}^k$ with $k = j + m + 1$, with $m \geqslant 0, k \geqslant 1$ non-negative integers, and $p_k \in R^j C R^m$. Then Germ$(p_k)$ contains a curve germ equivalent to the $A_{2k}$ singularity, which implies that the $RVT$ class $R^j C R^m$ consists of a single orbit.*

**Remark 3.6.** The letter $C$ in the above stands for a *critical point*. This notation will be explained in more detail in Section 4.1.

**Remark 3.7** *(Monster Tower is a fiber compactification of jet spaces).* The space of $k$-jets of functions $f : \mathbb{R} \to \mathbb{R}^2$, usually denoted by $J^k(\mathbb{R}, \mathbb{R}^2)$ is an open dense subset of $\mathcal{P}^k$. It is in this sense that a point $p \in \mathcal{P}^k$ is roughly speaking the $k$-jet of a curve in $\mathbb{R}^3$. Sections of the bundle

$$J^k\left(\mathbb{R}, \mathbb{R}^2\right) \to \mathbb{R} \times \mathbb{R}^2$$

are $k$-jet extensions of functions. Explicitly, given a vector-valued function $t \mapsto f(t) = (x(t), y(t))$ its $k$-jet extension is defined as

$$\left(t, f(t)\right) \mapsto \left(t, x(t), y(t), x'(t), y'(t), \ldots, x^{(k)}(t), y^{(k)}(t)\right).$$

Superscripts here denote the order of the derivative. It is an instructive exercise to show that for certain choices of fiber affine coordinates in $\mathcal{P}^k$, not involving critical directions, that our local charts will look like a copy of $J^k(\mathbb{R}, \mathbb{R}^2)$.

Another reason to look at curves is that it gives us a better picture of the overall behavior of an $RVT$ class. If one knows all the possible curve normal forms for a particular $RVT$ class, say $\omega$, then not only does one know how many orbits are within the class $\omega$, but one also knows how many orbits are within the regular prolongation of $\omega$. By regular prolongation of an $RVT$ class $\omega$ we mean the addition of only $R$'s to the end of the word $\omega$, i.e. the regular prolongation of $\omega$ is $\omega R \cdots R$. This method of using curves to classify $RVT$ classes was used in [19].

## 4. Tools and ideas involved in the proofs

Before we begin with the proofs we need to define the $RVT$ code for classifying orbits.

### 4.1. RC coding of points

**Definition 4.1.** A point $p_k \in \mathcal{P}^k$, where $p_k = (p_{k-1}, \ell)$ is called a *regular or critical point* if the line $\ell$ is a regular direction or a critical direction.

**Definition 4.2.** For $p_k \in \mathcal{P}^k$, $k \geqslant 1$, and $p_i = \pi_{k,i}(p_k)$, we write $\omega_i(p_k) = R$ if $p_i$ is a regular point and $\omega_i(p_k) = C$ if $p_i$ is a critical point. Then the word $\omega(p_k) = \omega_1(p_k) \cdots \omega_k(p_k)$ is called the $RC$ code for the point $p_k$. The number of letters within the $RC$ code for $p_k$ equals the level of the tower that the point lives in. Note that $\omega_1(p_k)$ is always equal to $R$ by Theorem 3.4.

So far we have not discussed how critical directions sit inside of $\Delta_k$. The following section will show that there is more than one kind of critical direction that can appear within the distribution $\Delta_k$.

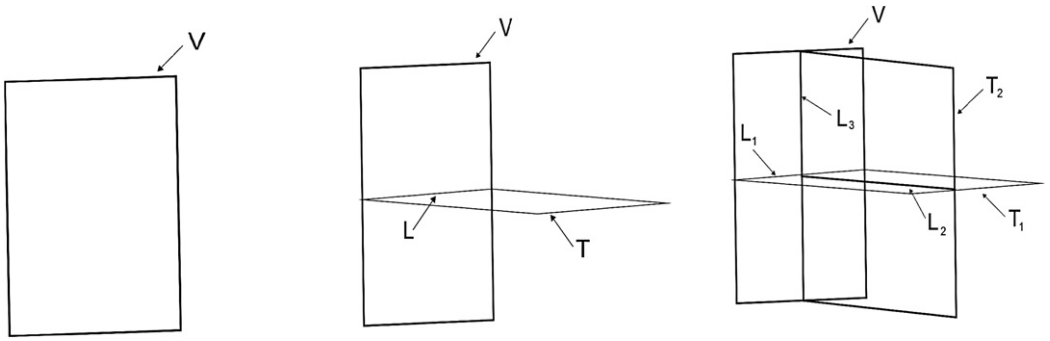


(A) Above a regular point (B) Above a vertical or tangency point (C) Above an $L$ point

**Fig. 2.** Arrangement of critical hyperplanes.

### 4.2. Baby Monsters

One can apply prolongation to any analytic $n$-dimensional manifold $F$ in place of $\mathbb{R}^n$. Start out with $\mathcal{P}^0(F) = F$ and take $\Delta_0^F = TF$. Then the prolongation of the pair $(F, \Delta_0^F)$ is $\mathcal{P}^1(F) = \mathbb{P}TF$ equipped with the rank $m$ distribution $\Delta_1^F \equiv (\Delta_0^F)^1$. By iterating this process $k$ times we end up with new the pair $(\mathcal{P}^k(F), \Delta_k^F)$, which is analytically diffeomorphic to $(\mathcal{P}^k(n-1), \Delta_k)$ [6].

Now, apply this process to the fiber $F_i(p_i) = \pi_{i,i-1}^{-1}(p_{i-1}) \subset \mathcal{P}^i$ through the point $p_i$ at level $i$. The fiber is an $(n-1)$-dimensional integral submanifold for $\Delta_i$. Prolonging, we see that $\mathcal{P}^1(F_i(p_i)) \subset \mathcal{P}^{i+1}$, and $\mathcal{P}^1(F_i(p_i))$ has the associated distribution $\delta_i^1 \equiv \Delta_1^{F_i(p_i)}$; that is,

$$\delta_i^1(q) = \Delta_{i+1}(q) \cap T_q\big(\mathcal{P}^1\big(F_i(p_i)\big)\big)$$

which is a hyperplane within $\Delta_{i+1}(q)$, for $q \in \mathcal{P}^1(F_i(p_i))$. When this prolongation process is iterated, we end up with the submanifolds

$$\mathcal{P}^j\big(F_i(p_i)\big) \subset \mathcal{P}^{i+j}$$

with the hyperplane subdistribution $\delta_i^j(q) \subset \Delta_{i+j}(q)$ for $q \in \mathcal{P}^j(F_i(p_i))$.

**Definition 4.3.** A *Baby Monster* born at level $i$ is a sub-tower $(\mathcal{P}^j(F_i(p_i)), \delta_i^j)$, for $j \geqslant 0$ within the ambient Monster Tower. If $q \in \mathcal{P}^j(F_i(p_i))$ then we will say that a Baby Monster born at level $i$ passes through $q$ and that $\delta_i^j(q)$ is a *critical hyperplane* passing through $q$, which was born at level $i$.

**Definition 4.4.** The *vertical plane* $V_k(q)$ is the critical hyperplane $\delta_k^0(q)$. We note that it is always one of the critical hyperplanes passing through $q$.

The following statement elucidates the geometric properties of critical directions.

**Theorem 4.1.** *A direction $\ell \subset \Delta_k$ is critical if and only if $\ell$ is contained in a critical hyperplane.*

### 4.3. Arrangements of critical hyperplanes for $n = 2$

Over any point $p_k$, at the $k$-th level of the Monster Tower, there is a total of three different hyperplane configurations for $\Delta_k$. These three configurations are shown in Figs. 2(a), 2(b), and 2(c).

Fig. 2(a) is the picture for $\Delta_k(p_k)$ when the $k$-th letter in the $RVT$ code for $p_k$ is the letter $R$. This means that the vertical hyperplane, labeled with a $V$, is the only critical hyperplane sitting inside of $\Delta_k(p_k)$. Fig. 2(b) is the picture for $\Delta_k(p_k)$ when the $k$-th letter in the $RVT$ code is either the letter $V$ or the letter $T$. This gives a total of two critical hyperplanes sitting inside of $\Delta_k(p_k)$ and one distinguished critical direction: one is the vertical hyperplane and the other is the tangency hyperplane, labeled by the letter $T$. The intersection of vertical and tangency hyperplanes gives a distinguished critical direction, which is labeled by the letter $L$. Now, Fig. 2(c) describes the picture for $\Delta_k(p_k)$ when the $k$-th letter in the $RVT$ code of $p_k$ is the letter $L$. Fig. 2(c) depicts this situation where there is now a total of three critical hyperplanes: one is the vertical hyperplane, and two tangency hyperplanes, labeled as $T_1$ and $T_2$. Now, because of the presence of these three critical hyperplanes we need to refine our notion of an $L$ direction and add two more distinct $L$ directions. These

three directions are labeled as $L_1$, $L_2$, and $L_3$. More details concerning the properties of these critical hyperplanes and their various configurations can be found in [6].

With the above picture in mind, we can now refine our $RC$ coding and define the $RVT$ code for points within the Monster Tower. Take $p_k \in \mathcal{P}^k$ and if $\omega_i(p_k) = C$ then we look at the point $p_i = \pi_{k,i}(p_k)$, where $p_i = (p_{i-1}, \ell_{i-1})$. Then depending on which critical hyperplane, or distinguished direction, contains $\ell_{i-1}$, we replace the letter $C$ by the letter $V$, $T$, $L$, $T_i$ for $i = 1, 2$, or $L_j$ for $j = 1, 2, 3$. One can see from the above geometric considerations that these critical letters must follow three simple *grammar rules*.

(1) The first one states that the initial letter in any $RVT$ code string must be the letter $R$. This is a consequence of Theorem 3.4.
(2) The second is that the letters $T$ or $L$, along with $T_i$ for $i = 1, 2$ and $L_j$ for $j = 1, 2, 3$, cannot immediately follow the letter $R$.
(3) The last one is that the letters $T_2$ and $L_j$ for $j = 1, 2, 3$ can only appear immediately after the letter $L = (L_1)$.

For the case of length 4 the letters $T_2$ and $L_j$ for $j = 2, 3$ can only appear immediately after the letter $L = (L_1)$. However, for a point of length larger than 4 we believe that this rule still holds. This fact will be investigated in a future work by one of the authors.

**Example 4.2** *(Examples of $RVT$ codes).* The following are examples of $RVT$ codes: $R \cdots R$, $RVVT$, $RVLT_2R$, and $RVLL_2$. The code $RTL$ is not allowed because the letter $T$ is preceded by the letter $R$ and the code $RLT_3$ is not allowed because the letter $L$ comes immediately after the letter $R$.

As a result, we see that each of the first four levels of the Monster Tower is made up of the following $RVT$ classes:

- Level 1:

  $R$.

- Level 2:

  $RR, RV$.

- Level 3:

  $RRR, RRV, RVR, RVV, RVT, RVL$.

- Level 4:

  $RRRR, RRRV$

  $RRRV, RRVV, RRVT, RRVL$

  $RVRR, RVRV, RVVR, RVVV, RVVT, RVVL$

  $RVTR, RVTV, RVTT, RVTL$

  $RVLR, RVLV, RVLT_1, RVLT_2, RVLL_1, RVLL_2, RVLL_3$.

**Remark 4.3.** As it was pointed out in [6] the symmetries, at any level in the Monster Tower preserve the critical hyperplanes. In other words, if $\Phi^k$ is a symmetry at level $k$ in the Monster Tower and $\delta_i^j$ is a critical hyperplane within $\Delta_k$ then $\Phi^k_*(\delta_i^j) = \delta_i^j$. As a result, the $RVT$ classes create a partition of the various points within any level of the Monster Tower, i.e., the $RVT$ classes are invariant under the *Diff*(3) action. More details about the properties of the various critical hyperplanes and distinguished critical directions can be found in [6].

Now, from the above configurations of critical hyperplanes section one might ask the following question: How does one "see" the two tangency hyperplanes that appear over an "$L$" point and where do they come from? This question was an important one to ask when trying to classify the number of orbits within the fourth level of the Monster Tower and to better understand the geometry of the tower. We will provide an example to answer this question, but before we do so we must discuss some details about a particular coordinate system called Kumpera–Rubin coordinates to help us do various computations within the Monster Tower.

### *4.4. Kumpera–Rubin coordinates*

When doing local computations in the tower (1), one needs to work with suitable coordinates. A good choice of coordinates was suggested by Kumpera and Ruiz [11] in the Goursat case, and later generalized by Kumpera and Rubin [12]

for multi-flags. A detailed description of the inductive construction of Kumpera–Rubin coordinates was given in [6] and is discussed in the example following this section, as well as in the proof of our level 3 classification. For the sake of clarity, we will highlight the coordinates' attributes through an example.

**Example 4.4** *(Constructing fiber affine coordinates in $\mathcal{P}^2$).*

**Level one:** Consider the pair $(\mathbb{R}^3, T\mathbb{R}^3)$ and let $(x, y, z)$ be local coordinates on $\mathbb{R}^3$. The triple of 1-forms $\{dx, dy, dz\}$ forms a coframe of $T\mathbb{R}^3$. Any line $\ell_0$ in the tangent space at $p_0 \in \mathbb{R}^3$ has projective coordinates $[dx|_{\ell_0} : dy|_{\ell_0} : dz|_{\ell_0}]$. Since the affine group of $\mathbb{R}^3$, which is contained in $Diff(3)$, acts transitively on $\mathbb{P}(T\mathbb{R}^3)$, we can fix $p_0 = (0, 0, 0)$ $(= \mathbf{0})$ and $\ell_0 = span\{\frac{\partial}{\partial x}\}$. Thus $dx|_{\ell_0} \neq 0$ and we introduce fiber affine coordinates $[1 : dy/dx : dz/dx]$ where,

$$u = \frac{dy}{dx}, \qquad v = \frac{dz}{dx}.$$

The Pfaffian system describing the prolonged distribution $\Delta_1$ on $\mathcal{P}^1 = \mathbb{R}^3 \times \mathbb{P}^2$ is

$$\{dy - udx = 0, dz - vdx = 0\} = \Delta_1 \subset T\mathcal{P}^1.$$

At the point $p_1 = (p_0, \ell_0) = (x, y, z, u, v) = (0, 0, 0, 0, 0)$ the distribution is the linear subspace

$$\Delta_{1\,(0,0,0,0,0)} = \{dy = 0, dz = 0\}.$$

The triple of 1-forms $\{dx, du, dv\}$ forms a local coframe for $\Delta_1$ near $p_1 = (p_0, \ell_0)$. The fiber, $F_1(p_1) = \pi_{1,0}^{-1}(p_0)$, is given by $x = y = z = 0$. The 2-plane of critical directions ("bad-directions") is thus spanned by $\frac{\partial}{\partial u}, \frac{\partial}{\partial v}$.

The reader may have noticed that we could have chosen any regular direction at level 1 instead, e.g. $\frac{\partial}{\partial x} + a\frac{\partial}{\partial u} + b\frac{\partial}{\partial v}$ and centered our chart at it. Again, this is because all regular directions at level one are pairwise equivalent by a symmetry transformation.

**Remark 4.5.** Let us remind the reader that $\mathcal{P}^1$ is diffeomorphic to $\mathbb{R}^3 \times \mathbb{P}^2$ but $\mathcal{P}^k$ is not a trivial bundle over $\mathbb{R}^3$ if $k \geqslant 2$ (cf. [6, Section 2]).

**Level two ($RV$ points):** Any line $\ell_1 \subset \Delta_1(p_1')$, for $p_1'$ near $p_1$, will have projective coordinates

$$[dx|_{\ell_1} : du|_{\ell_1} : dv|_{\ell_1}].$$

If we choose a critical direction, say $\ell_1 = span\{\frac{\partial}{\partial u}\}$, then $du(\frac{\partial}{\partial u}) = 1$ and we can center our chart at the direction $\ell_1$ and the chart is given by the projective coordinates $[\frac{dx}{du} : 1 : \frac{dv}{du}]$. *We will show below that any two critical directions are equivalent and therefore such a choice does not result in any loss of generality*. We introduce new fiber affine coordinates

$$u_2 = \frac{dx}{du}, \qquad v_2 = \frac{dy}{du},$$

and the distribution $\Delta_2$ will be described in this chart as

$$\begin{aligned}\Delta_2 = \{&dy - udx = 0, dz - vdx = 0,\\ &dx - u_2du = 0, dv - v_2du = 0\} \subset T\mathcal{P}^2.\end{aligned}$$

**Level three (the tangency hyperplanes over an $L$ point):** We take $p_3 = (p_2, \ell_2) \in RVL$ with $p_2$ as in the level two discussion. We now look at local affine coordinates near the point $p_2$. We will show that inside of this chart that the tangency hyperplane $T_1$ in $\Delta_3(p_3)$ is the critical hyperplane $\delta_2^1(p_3) = span\{\frac{\partial}{\partial v_2}, \frac{\partial}{\partial v_3}\}$ and the tangency hyperplane $T_2$ is the critical hyperplane $\delta_1^2(p_3) = span\{\frac{\partial}{\partial v_2}, \frac{\partial}{\partial u_3}\}$.

We begin with the local coordinates near $p_3$. Let us first recall that the distribution $\Delta_2$ is coframed by $\{du, du_2, dv_2\}$ in this case. Within $\Delta_2$ the vertical hyperplane is given by $du = 0$ and the tangency hyperplane by $du_2 = 0$. The point $p_3 = (p_2, \ell)$ with $\ell$ being an $L$ direction means that both $du|_\ell = 0$ and $du_2|_\ell = 0$. This means that the only choice for local coordinates near $p_3$ is given by $[\frac{du}{dv_2} : \frac{du_2}{dv_2} : 1]$. As a result, the fiber coordinates at level 3 are

$$u_3 = \frac{du}{dv_2}, \qquad v_3 = \frac{du_2}{dv_2}$$

and the distribution $\Delta_3$ will be described in this chart as

$$\begin{aligned}\Delta_3 = \{&dy - udx = 0, dz - vdx = 0,\\ &dx - u_2du = 0, dv - v_2du = 0,\\ &du - u_3dv_2 = 0, du_2 - v_3dv_2 = 0\} \subset T\mathcal{P}^3.\end{aligned}$$

With this in mind, we are ready to determine how the two tangency hyperplanes are situated within $\Delta_3$.

- **Showing $T_1$ is equal to $\delta_2^1(p_3)$:** First we note that $p_3 = (x, y, z, u, v, u_2, v_2, u_3, v_3) = (0, 0, 0, 0, 0, 0, 0, 0, 0)$ with $u = \frac{dy}{dx}$, $v = \frac{dz}{dx}$, $u_2 = \frac{dx}{du}$, $v_2 = \frac{dv}{du}$, $u_3 = \frac{du}{dv_2}$, $v_3 = \frac{du_2}{dv_2}$. With this in mind, we start by looking at the vertical hyperplane $V_2(p_2) \subset \Delta_2(p_2)$ and prolong the fiber $F_2(p_2)$ associated to $V_2(p_2)$ and see that

$$\begin{aligned}\mathcal{P}^1\big(F_2(p_2)\big) = \mathbb{P}V_2 &= \big(p_1, u_2, v_2, [du : du_2 : dv_2]\big) = \big(p_1, u_2, v_2, [0 : a : b]\big)\\ &= \left(p_1, u_2, v_2, \left[0 : \frac{a}{b} : 1\right]\right) = (p_1, u_2, v_2, 0, v_3)\end{aligned}$$

where $a, b \in \mathbb{R}$ with $b \neq 0$. One sees that $\Delta_3$, in a neighborhood of $p_3$, is given by

$$\Delta_3 = span\left\{u_3 X^{(2)} + v_3 \frac{\partial}{\partial u_2} + \frac{\partial}{\partial v_2}, \frac{\partial}{\partial u_3}, \frac{\partial}{\partial v_3}\right\}$$

with $X^{(2)} = u_2 X_1^{(1)} + \frac{\partial}{\partial u} + v_2 \frac{\partial}{\partial v}$ and $X^{(1)} = u\frac{\partial}{\partial y} + v\frac{\partial}{\partial z} + \frac{\partial}{\partial x}$ and that $T_{p_3}(\mathcal{P}^1(F_2(p_2))) = span\{\frac{\partial}{\partial u_2}, \frac{\partial}{\partial v_2}, \frac{\partial}{\partial v_3}\}$. From the definition of $\delta_i^j$ we have that

$$\delta_2^1(p_3) = \Delta_3(p_3) \cap T_{p_3}\big(\mathcal{P}^1\big(F_2(p_2)\big)\big)$$

which gives that

$$\delta_2^1(p_3) = span\left\{\frac{\partial}{\partial v_2}, \frac{\partial}{\partial v_3}\right\}.$$

Now, since $V_3(p_3) \subset \Delta_3(p_3)$ is given by $V_3(p_3) = span\{\frac{\partial}{\partial u_3}, \frac{\partial}{\partial v_3}\}$ we see, based upon Fig. 2(c), that $T_1 = \delta_2^1(p_3)$.

- **Showing $T_2$ is equal to $\delta_1^2(p_3)$:** We begin by looking at $V_1(p_1) \subset \Delta_1(p_1)$ and at the fiber $F_1(p_1)$ associated to $V_1(p_1)$. When we prolong the fiber space we see that

$$\begin{aligned}\mathcal{P}^1\big(F_1(p_1)\big) = \mathbb{P}V_1 &= \big(0, 0, 0, u, v, [dx : du : dv]\big) = \big(0, 0, 0, u, v, [0 : a : b]\big)\\ &= \left(0, 0, 0, u, v, \left[0 : 1 : \frac{b}{a}\right]\right) = (0, 0, 0, u, v, 0, v_2)\end{aligned}$$

where $a, b \in \mathbb{R}$ with $a \neq 0$. Now $\Delta_2$, in a neighborhood of $p_2$, is given by

$$\Delta_2 = span\left\{u_2 X^{(1)} + \frac{\partial}{\partial u} + v_2 \frac{\partial}{\partial v}, \frac{\partial}{\partial u_2}, \frac{\partial}{\partial v_2}\right\}$$

and at the same time $T_{p_2}(\mathcal{P}^1(F_1(p_1))) = span\{\frac{\partial}{\partial u}, \frac{\partial}{\partial v}, \frac{\partial}{\partial v_2}\}$. This gives

$$\delta_1^1(p_2) = \Delta_2(p_2) \cap T_{p_2}\big(\mathcal{P}^1\big(F_1(p_1)\big)\big)$$

and we have in a neighborhood of $p_2$ that

$$\delta_1^1 = span\left\{u_2 X^{(1)} + \frac{\partial}{\partial u} + v_2 \frac{\partial}{\partial v}, \frac{\partial}{\partial v_2}\right\}.$$

Now, in order to figure out what $\delta_1^2(p_3)$ is we need to prolong the fiber $F_1(p_1)$ twice and then look at the tangent space at the point $p_3$. We see that

$$\begin{aligned}\mathcal{P}^2\big(F_1(p_1)\big) = \mathbb{P}\delta_1^1 &= \big(0, 0, 0, u, v, 0, v_2, [du : du_2 : dv_2]\big)\\ &= \big(0, 0, 0, u, v, 0, v_2, [a : 0 : b]\big)\\ &= \left(0, 0, 0, u, v, 0, v_2, \left[\frac{a}{b} : 0 : 1\right]\right)\\ &= (0, 0, 0, u, v, 0, v_2, u_3, 0)\end{aligned}$$

then since

$$\delta_1^2(p_3) = \Delta_3(p_3) \cap T_{p_3}\big(\mathcal{P}^2\big(F_1(p_1)\big)\big)$$

with $\Delta_3(p_3) = span\{\frac{\partial}{\partial v_2}, \frac{\partial}{\partial u_3}, \frac{\partial}{\partial v_3}\}$ and $T_{p_3}(\mathcal{P}^2(F_1(p_1))) = span\{\frac{\partial}{\partial u}, \frac{\partial}{\partial v}, \frac{\partial}{\partial v_2}, \frac{\partial}{\partial u_3}\}$ then

$$\delta_1^2(p_3) = span\left\{\frac{\partial}{\partial v_2}, \frac{\partial}{\partial u_3}\right\}$$

and from looking at Fig. 2(c) one can see that $T_2 = \delta_1^2(p_3)$.

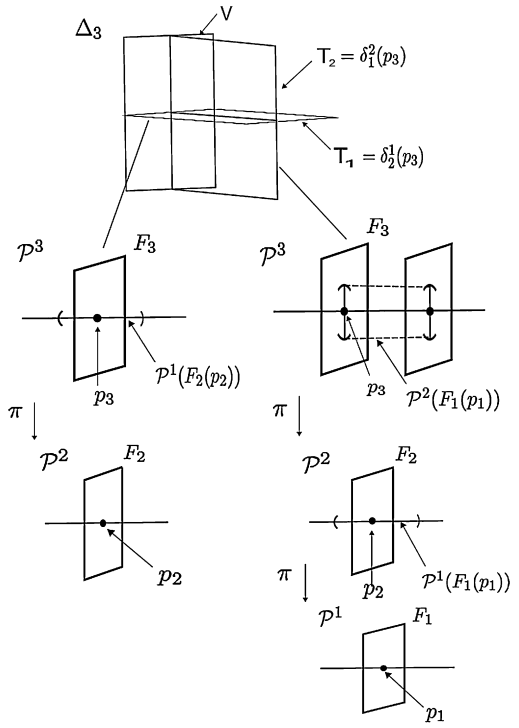


**Fig. 3.** Critical hyperplane configuration over $p_3 \in RVL$.

**Remark 4.6.** The above example, along with Fig. 3, gives some reasoning for why a critical hyperplane, which is not the vertical one, is called a *tangency* hyperplane. Also, in Fig. 3 we have drawn the submanifolds $\mathcal{P}^1(F_2(p_2))$ and $\mathcal{P}^1(F_1(p_1))$ to reflect the fact that they have some component which is tangent to the manifolds $\mathcal{P}^3$ and $\mathcal{P}^2$ respectively and that their other component is tangent to the vertical space. At the same time, they are drawn to show the fact that $\mathcal{P}^2(F_1(p_1))$ is tangent to the $\frac{\partial}{\partial u_3}$ direction while $\mathcal{P}^1(F_2(p_2))$ is tangent to the $\frac{\partial}{\partial v_3}$ direction. Another reason for why we use this terminology is because it was first introduced in the context of the $n = 1$ Monster Tower to distinguish those critical directions that were not vertical, and that were actually contained in the tangent bundle of $\mathcal{P}^k(1)$ [19].

### *4.5. Semigroup of a curve*

An important piece of information that we need to present is some terminology relating to curves. Some of the following properties about curve germs are presented in greater detail in [6].

**Definition 4.5.** The *order* of an analytic curve germ $f(t) = \sum_{i \geqslant 0} a_i t^i$ is the smallest integer $i$ such that $a_i \neq 0$. We write $\mathrm{ord}(f)$ for this (non-negative) integer. The *multiplicity* of a curve germ $\gamma : (\mathbb{R}, 0) \to (\mathbb{R}^n, 0)$, denoted $mult(\gamma)$, is the minimum of the orders of its coordinate functions $\gamma_i(t)$ relative to any coordinate system vanishing at $p$.

**Definition 4.6.** A curve germ is said to be *well parameterized* if $\gamma$ cannot be written in the form $\gamma = \sigma \circ \tau$ where $\tau : (\mathbb{R}, 0) \to (\mathbb{R}, 0)$ with $\tau'(0) = 0$ [23].

**Definition 4.7.** If $\gamma : (\mathbb{R}, 0) \to (\mathbb{R}^n, 0)$ is a well-parameterized curve germ, then its *semigroup* is the collection of positive integers $\mathrm{ord}(P(\gamma(t)))$ as $P$ varies over analytic functions of $n$ variables vanishing at 0.

Because $\mathrm{ord}(PQ(\gamma(t))) = \mathrm{ord}(P(\gamma(t))) + \mathrm{ord}(Q(\gamma(t)))$ the curve semigroup is indeed an algebraic semigroup, i.e. a subset of $\mathbb{N}$ closed under addition. The semigroup of a well-parameterized curve is a basic diffeomorphism invariant of the curve.

**Remark 4.7.** Arnol'd pointed out in [1] that one can use the semigroup of a curve germ as a tool to see if it is $RL$ equivalent to a simpler curve germ. Details and examples about semigroup calculations can be found within [1] as well as in [23]. We do though provide the following short example to help the reader.

**Example 4.8.** Let $\gamma_1(t) = (t^3, t^5, t^7)$ and $\gamma_2(t) = (t^3, t^5+t^6+t^8, t^7+t^9)$ be curve germs defined for $t$ in an open interval about zero. Both of the curves $\gamma_1$ and $\gamma_2$ generate the same semigroup. In this case the semigroup is the set $S = \{3, [4], 5, 6, 7, \ldots\}$ where the binary operation is addition. The numbers 3, 5, 6, and so on are elements of this semigroup while the bracket around the number 4 means that it is not an element of $S$. When we write "$\cdots$" after the number 7 it means that every positive integer after 7 is an element in our semigroup. Arnol'd points out that the terms in the semigroup tell us which powers of $t$ we can eliminate from the curve. This means that every term, $t^i$ for $i \geqslant 7$, can be eliminated, except for the $t^7$ term in the last component function, from the above power series expansion for the component functions $x(t)$, $y(t)$, and $z(t)$ by a change of variables given by $(x, y, z) \mapsto (x + f(x, y, z), y + g(x, y, z), z + h(x, y, z))$. Since the numbers 6, 8, and 9 are included in the semigroup it means that we can use a combination of $RL$ equivalences to kill the $t^6$ and $t^8$ terms in the $y$ component and the $t^9$ term in the $z$ component of $\gamma_2$. This means that the curve germs $\gamma_1$ and $\gamma_2$ are in fact $RL$ equivalent.

### *4.6. The points-to-curves and back philosophy*

The idea is to translate the problem of classifying orbits in the tower (1) into an equivalent classification problem for finite jets of space curves. Here we are going to mention some highlights of this approach, we will refer the diligent reader to [6] to check the technical details.

For any $p \in \mathcal{P}^k(n)$ we associate the set $Germ(p)$ and look at the operation of $k$-fold prolongation applied to curve germs in $Germ(p)$. This yields immersed curves at level $k$ in the Monster Tower, and tangent to some line $\ell$ having nonconstant projection onto the base manifold $\mathbb{R}^3$. Such sets of *good directions* were christened *regular* in [6], and within each subspace $\Delta_k$ they form an open dense set. A *bad direction* $\ell_*$, or *critical direction* in the terminology of [6], are those directions which will project down to a point under the differential of the bundle projection map. The set of critical directions within each $\Delta_k$ is a finite union of planes. Symmetries of $\mathcal{P}^k$ do preserve the different types of directions.

In [6] it was proved that $Germ(p)$ is always non-empty. Consider now the set valued map $p \mapsto Germ(p)$. One can prove that $p \sim q$ iff $Germ(p) \sim Germ(q)$. An immediate and yet useful consequence of this fact is the following:

**Lemma 4.9** *(Fundamental lemma of points-to-curves approach). Let $\Omega$ be a subset of $\mathcal{P}^k(n)$ and suppose for each $p \in \Omega$ that $Germ(p)$ contains only a finite number of equivalence classes of curve germs. Then the set $\Omega$ is comprised of only a finite number of orbits.*

### *4.7. The isotropy method*

The last piece of information that we need to present before we begin the proofs section is the isotropy method. This technique is used to classify points at the fourth level of the Monster Tower. This is because the curve approach failed to provide us with nice and clean normal forms for the various $RVT$ classes at the fourth level of the tower. We provide a specific example of how the curve approach breaks down at level 4 in the proofs section. Suppose we want to look at a particular $RVT$ class, at the $k$-th level, given by $\omega$ (a word of length $k$) and we want to see how many orbits there are. Suppose as well that we understand its projection $\pi_{k,k-1}(\omega)$ one level down, which decomposes into $N$ orbits. Choose representative points $p_i$, $i = 1, \ldots, N$, for the $N$ orbits in $\pi_{k,k-1}(\omega)$, and consider the group $G_{k-1}(p_i)$ of level $k-1$ symmetries that fix $p_i$. This group is called the *isotropy group of* $p_i$. Since elements $\Phi^{k-1}$ of the isotropy group fix $p_i$, their prolongations $\Phi^k = (\Phi^{k-1}, \Phi^{k-1}_*)$ act on the fiber over $p_i$. Under the action of the isotropy group the fiber decomposes into some number $n_i \geqslant 1$ (possibly infinite) of orbits. Summing up, we find that $\omega$ decomposes into $\sum_{i=1}^{N} n_i \geqslant N$ orbits. This will tell us how many orbits there are for the class $\omega$.

This is the theory. Now we need to explain how one actually prolongs diffeomorphisms in practice. Since the manifold $\mathcal{P}^k$ is a type of fiber compactification of $J^k(\mathbb{R}, \mathbb{R}^2)$, it is reasonable to expect that the prolongation of diffeomorphisms from the base $\mathbb{R}^3$ should be similar to what one does when prolonging point symmetries from the theory of jet spaces. See specifically [7] and [20].

Given a point $p_k \in \mathcal{P}^k$ and a map $\Phi \in Diff(3)$ we would like to write explicit formulas for $\Phi^k(p_k)$. Coordinates of $p_k$ can be made explicit. Now take any curve $\gamma(t) \in Germ(p_k)$, and consider the prolongation of $\Phi \circ \gamma(t)$. The coordinates of $\Phi^k(p_k)$ are exactly the coordinates of $(\Phi \circ \gamma)^{(k)}(0) = \Phi^k(\gamma^k(0))$. Moreover the resulting point is independent of the choice of $\gamma \in Germ(p)$ and therefore we can act as if a curve has been chosen when performing actual computations.

## 5. Proofs

Now we are ready to prove Theorem 3.2. We start at level 1 of the tower and work our way up to level 4. At each level of the tower we classify the number of orbits within each $RVT$ class that appears at that particular level. In this section we show how the various methods and tools from the previous section are used in the classification procedure. Unfortunately we do not have space to present all the details for the determination of all orbits within each $RVT$ class at both levels 3 and 4 of the Monster Tower. We will instead present a few instructive examples which will illustrate how the determination of the number of orbits in the remaining classes works.

### 5.1. The classification of points at level 1 and level 2

Theorem 3.4 tells us that all points at the first level of the tower are equivalent, giving that there is a single orbit. For level 2 there are only two possible $RVT$ codes: $RR$ and $RV$. Again, any point in the class $RR$ is a Cartan point and by Theorem 3.4 consists of only one orbit. The class $RV$ consists of a single orbit by Theorem 3.5.

### 5.2. The classification of points at level 3

There is a total of six distinct $RVT$ classes at level three in the Monster Tower. We begin with the class $RRR$.

*The class $RRR$*: Any point within the class $RRR$ is a Cartan point and Theorem 3.4 gives that there is only one orbit within this class.

*The classes $RVR$ and $RRV$*: From Theorem 3.5 we know that any point within the class $RVR$ has a single orbit, which is represented by the point $\gamma^3(0)$ where $\gamma$ is the curve $\gamma(t) = (t^2, t^3, 0)$. Similarly, the class $RRV$ has a single orbit, which is represented by the point $\tilde{\gamma}^3(0)$ where $\tilde{\gamma}(t) = (t^2, t^5, 0)$.

Before we continue, we need to pause and provide some framework to help us with the classification of the remaining $RVT$ codes.

*Setup for classes of the form $RVC$*: We set up coordinates $x, y, z, u, v, u_2, v_2$ for a point in the class $RV$ as in Section 4.4. Then for $p_2 \in RV$ we have $\Delta_2(p_2) = span\{\frac{\partial}{\partial u}, \frac{\partial}{\partial u_2}, \frac{\partial}{\partial v_2}\}$ where $p_2 = (x, y, z, u, v, u_2, v_2) = (0, 0, 0, 0, 0, 0, 0)$, and for any point $p_3 \in RVC \subset \mathcal{P}^3$ that $p_3 = (p_2, \ell_2) = (p_2, [du|_{\ell_2} : du_2|_{\ell_2} : dv_2|_{\ell_2}])$. Since the point $p_2$ is in the class $RV$ we see that if $du = 0$ along $\ell_2$ then $p_3 \in RVV$. If $du_2 = 0$ with $du \neq 0$ along $\ell_2$ then $p_3$ will be an element of the class $RVT$, and if $du = 0$ and $du_2 = 0$ along $\ell_2$ that $p_3 \in RVL$. With this in mind, we are ready to continue with the classification.

*The class $RVV$*: Let $p_3 \in RVV$ and let $\gamma \in Germ(p_3)$. We prolong $\gamma$ two times and write $\gamma^2(t) = (x(t), y(t), z(t), u(t), v(t), u_2(t), v_2(t))$. We look at the component functions $u(t)$, $u_2(t)$, and $v_2(t)$. Since these component functions are analytic we can set $u(t) = \Sigma_i a_i t^i$, $u_2(t) = \Sigma_j b_j t^j$, and $v_2(t) = \Sigma_k c_k t^k$. We note that the reason for looking only at these terms is because $\delta_2(p_2)$ is spanned by the collection of vectors $\{\frac{\partial}{\partial u}, \frac{\partial}{\partial u_2}, \frac{\partial}{\partial v_2}\}$. Now, since $\gamma^2(t)$ needs to be tangent to the vertical hyperplane in $\Delta_3$ then $\frac{d}{dt}\gamma^2|_{t=0}$ must be a proper vertical direction in $\Delta_3$; that is $\frac{d}{dt}\gamma^2|_{t=0}$ is not an $L$ direction. Since $\Delta_3$ is coframed by $du$, $du_2$, and $dv_2$, we must have that $du = 0$ and $du_2 \neq 0$ along $\frac{d}{dt}\gamma^2|_{t=0}$. This imposes the condition for the functions $u(t)$ and $u_2(t)$ that $a_1 = 0$ and $b_1 \neq 0$, but the coefficient $c_1$ in $v_2(t)$ may or may not be zero. Also it must be true that $a_2 \neq 0$ or else the curve $\gamma$ will not be in the set $Germ(p_3)$. We first look at the case when $c_1 \neq 0$.

- *Case* 1, $c_1 \neq 0$: From looking at the one-forms that determine $\Delta_2$, we see that in order for the curve $\gamma^3$ to be integral to this distribution, the component functions for $\gamma^3$ must satisfy the following relations:

$$\dot{y}(t) = u(t)\dot{x}(t), \qquad \dot{z}(t) = v(t)\dot{x}(t),$$
$$\dot{x}(t) = u_2(t)\dot{u}(t), \qquad \dot{v}(t) = v_2(t)\dot{u}(t).$$

  We start with the expressions for $\dot{x}(t)$ and $\dot{v}(t)$ and see, based upon what we know about $u(t)$, $u_2(t)$, and $v_2(t)$, that $x(t) = \frac{2a_2b_1}{3}t^3 + \cdots$ and $v(t) = \frac{2a_2c_1}{3}t^3 + \cdots$. We can then use this information to help us find $y(t)$ and $z(t)$. This gives us $y(t) = \frac{2a_2^2b_1}{5}t^5 + \cdots$ and $z(t) = \frac{4a_2^2b_1c_1}{3}t^7 + \cdots$. Now, we know what the first nonvanishing coefficients are for the curve $\gamma(t) = (x(t), y(t), z(t))$ and we want to determine the simplest curve that $\gamma$ must be equivalent to. In order to do this we will first look at the semigroup for the curve $\gamma$. In this case the semigroup is given by $S = \{3, [4], 5, 6, 7, \ldots\}$. This means that every term, $t^i$ for $i \geqslant 7$, can be eliminated from the above power series expansion for the component functions $x(t)$, $y(t)$, and $z(t)$ by a change of variables. With this in mind, after we rescale the leading coefficients for each of the components of $\gamma$, we end up with

$$\gamma(t) = \big(x(t), y(t), z(t)\big) \sim \big(\tilde{x}(t), \tilde{y}(t), \tilde{z}(t)\big) = \big(t^3 + \alpha t^4, t^5, t^7\big).$$

  We now want to see if we can eliminate the $\alpha$ term, if it is nonzero. To do this we will use a combination of reparametrization techniques along with semigroup arguments. Use the reparametrization $t = T(1 - \frac{\alpha}{3}T)$ and we get that $\tilde{x}(T) = T^3(1 - \frac{\alpha}{3}T)^3 + T^4(1 - \frac{\alpha}{3}T)^4 + \cdots = T^3 + O(T^5)$. This gives us that $(\tilde{x}(T), \tilde{y}(T), \tilde{z}(T)) = (T^3 + O(T^5), T^5 + O(T^6), T^7 + O(T^8))$. At the same time we can use the semigroup to eliminate all the terms of degree 5 or higher. As a result, these arguments show that $(\tilde{x}(T), \tilde{y}(T), \tilde{z}(T)) \sim (T^3, T^5, T^7)$. This means that our original $\gamma$ is equivalent to the curve $(t^3, t^5, t^7)$.
- *Case* 2, $c_1 = 0$: By repeating an argument similar to the above one, we will end up with $\gamma(t) = (x(t), y(t), z(t)) = (\frac{2a_2b_1}{3}t^3 + \cdots, \frac{2a_2^2b_1}{5}t^5 + \cdots, \frac{a_2^2b_1c_2}{8}t^8 + \cdots)$. Note that $c_2$ may or may not be equal to zero. This gives that the semigroup for the curve $\gamma$ is $S = \{3, [4], 5, 6, [7], 8, \ldots\}$ and that our curve $\gamma$ is such that

$$\gamma(t) = \big(x(t), y(t), z(t)\big) \sim \big(\tilde{x}(t), \tilde{y}(t), \tilde{z}(t)\big) = \big(t^3 + \alpha_1 t^4 + \alpha_2 t^7, t^5 + \beta t^7, 0\big).$$

  Again, we want to know if we can eliminate the $\alpha_i$ and $\beta$ terms. First we focus on the $\alpha_i$ terms in $\tilde{x}(t)$. We use the reparametrization given by $t = T(1 - \frac{\alpha_1}{3}T)$ to give us $\tilde{x}(T) = T^3 + \alpha_2' T^7 + O(T^8)$. Then to eliminate the $\alpha_2'$ term we use

the reparametrization given by $T = S(1 - \frac{\alpha'}{3}S^4)$ to give $\tilde{x}(S) = S^3 + O(S^8)$. We now turn our attention to the $\tilde{y}$ function. Because of our two reparametrizations we get that $\tilde{y}$ is of the form $\tilde{y}(S) = S^5 + \beta' S^7$. To get rid of the $\beta'$ term we simply use the rescaling given by $S \mapsto \frac{1}{\sqrt{|\beta'|}}S$ and then use the scaling diffeomorphism given by $(x, y, z) \mapsto (|\beta'|^{\frac{3}{2}}x, |\beta'|^{\frac{5}{2}}y, z)$ to give us that $\gamma$ is equivalent to either $(t^3, t^5 + t^7, 0)$ or $(t^3, t^5 - t^7, 0)$. Note that the above calculations were done under the assumption that $\beta \neq 0$. If $\beta = 0$ then we see, using similar calculations as above, that we get the normal form $(t^3, t^5, 0)$. This means that there is a total of 4 possible normal forms that represent the points within the class $RVV$. It is tempting, at first glance, to believe that these curves are all inequivalent. However, it can be shown that the 3 curves $(t^3, t^5 + t^7, 0)$, $(t^3, t^5 - t^7, 0)$, and $(t^3, t^5, 0)$ are actually equivalent. It is not very difficult to show this equivalence, but it does amount to rather messy calculation. *As a result, the techniques used to show this equivalence are outlined in Appendix* A.2.

This means that the possible normal forms are: $\gamma_1(t) = (t^3, t^5, t^7)$ and $\gamma_2(t) = (t^3, t^5, 0)$. We will show that these two curves are inequivalent. One possibility is to look at the semigroups that each of these curves generates. The curve $\gamma_1$ has the semigroup $S_1 = \{3, [4], 5, 6, 7, \ldots\}$, while the curve $\gamma_2$ has the semigroup $S_2 = \{3, [4], 5, 6, [7], 8, \ldots\}$. Since the semigroup of a curve is an invariant of the curve and the two curves generate different semigroups the two curves must be inequivalent. In [6] there was another technique used to check and see whether or not these two curves are equivalent. We will now present this alternative of showing that the two curves $\gamma_1$ and $\gamma_2$ are inequivalent.

One can see that the curve $(t^3, t^5, 0)$ is a planar curve and in order for the curve $\gamma_1$ to be equivalent to the curve $\gamma_2$ we must be able to find a way to turn $\gamma_1$ into a planar curve. More precisely, we need to find a change of variables and/or a reparametrization which will make the third component function of $\gamma_1$ zero. If it were true that $\gamma_1$ is $RL$ equivalent a planar curve, then $\gamma_1$ must lie in an embedded surface in $\mathbb{R}^3$ (or embedded surface germ), say $M$. This means there exists a local defining function at each point on the manifold $M$. Let the local defining function near the origin be the real analytic function $f : \mathbb{R}^3 \to \mathbb{R}$. Since $\gamma_1$ is on $M$, then $f(\gamma_1(t)) = 0$ for all $t$ near zero. However, when one looks at the individual terms in the Taylor series expansion of $f$ composed with $\gamma_1$ there will be nonzero terms which will show up and give that $f(\gamma_1(t)) \neq 0$ for all $t$ near zero, which creates a contradiction. This tells us that $\gamma_1$ cannot be equivalent to any planar curve near $t = 0$. As a result, there is a total of two inequivalent normal forms for the class $RVV$: $(t^3, t^5, t^7)$ and $(t^3, t^5, 0)$. When we prolong $\gamma_1$ and $\gamma_2$ to the third level in the tower we end up with $\gamma_1^3(0) = \gamma_2^3(0)$, which means that there is only one orbit within the class $RVV$.

The remaining classes $RVT$ and $RVL$ are proved in an almost identical manner using the above ideas and techniques. As a result, we will omit the proofs and leave them to the reader.

With this in mind, we are now ready to move on to the fourth level of the tower. We initially tried to tackle the problem of classifying the orbits at the fourth level by using the curve approach from the third level. Unfortunately, the curve approach became a bit too unwieldy to determine what the normal forms were for the various $RVT$ classes. The problem was simply this: when we looked at the semigroup for a particular curve in a number of the $RVT$ classes at the fourth level, there were too many *gaps* corresponding semigroup. The first occurring class, according to codimension, in which this occurred was the class $RVVV$. This turns the equivalence problem of curve germs computationally hard.

**Example 5.1** *(The semigroups for the class RVVV).* Let $p_4 \in RVVV$, and for $\gamma \in Germ(p_4)$ let $\gamma^3(t) = (x(t), y(t), z(t), u(t), v(t), u_2(t), v_2(t), u_3(t), v_3(t))$ with $u = \frac{dy}{dx}$, $v = \frac{dz}{dx}$, $u_2 = \frac{dx}{du}$, $v_2 = \frac{dv}{du}$, $u_3 = \frac{du}{du_2}$, $v_3 = \frac{dv_2}{du_2}$. Since $\gamma^4(0) = p_4$ we must have that $\gamma^3(t)$ is tangent to the vertical hyperplane within $\Delta_3$, which is coframed by $\{du_2, du_3, dv_3\}$. One can see that $du_2 = 0$ along $\frac{d}{dt}\gamma^3|_{t=0}$. Then, looking at the relevant component functions at the fourth level, we set $u_2(t) = \Sigma_i a_i t^i$, $u_3(t) = \Sigma_j b_j t^j$, $v_3(t) = \Sigma_k c_k t^k$ where we must have $a_1 = 0$, $a_2 \neq 0$, $b_1 \neq 0$, and $c_1$ may or may not be equal to zero. When we go from the fourth level back down to level zero we end up with $\gamma(t) = (t^5 + O(t^{11}), t^8 + O(t^{11}), O(t^{11}))$. If $c_1 \neq 0$, then we get $\gamma_1(t) = (t^5 + O(t^{12}), t^8 + O(t^{12}), t^{11} + O(t^{12}))$ and the semigroup for this curve is $S = \{5, [6], [7], 8, [9], 10, 11, [12], 13, [14], 15, 16, [17], 18, \ldots\}$. If $c_1 \neq 0$, then we get $\gamma_2(t) = (t^5 + O(t^{12}), t^8 + O(t^{12}), O(t^{12}))$ and the semigroup for this curve is $S = \{5, [6], [7], 8, [9], 10, [11], [12], 13, [14], 15, 16, [17], 18, [19], 20, 21, [22], 23, \ldots\}$. This shows there is a larger number of gaps in our semigroups and meant that we could not eliminate the various terms as easily in the various component functions of $\gamma_1$ and $\gamma_2$. As a result, it became impractical to work strictly using the curve approach. This meant that we had to look at a different approach to the classification problem. These types of issues are why we needed to develop a new approach and lead us to work with the isotropy method.

### 5.3. The classification of points at level 4

In classifying the points within the fourth level of the Monster Tower we worked almost exclusively with the isotropy method. While this method proved to be very effective in determining the number of orbits, we unfortunately do not present all the calculations using this technique. This is because the calculations can be lengthy and because of how many different possible $RVT$ codes there are at level 4. So we will present the proof for the classification of the class $RVVV$ as an example of how the isotropy method works.

*The class RVVV*: Before we get started, we will summarize the main idea of the following calculation. Our goal is to determine the number of orbits within the class $RVVV$. Let $p_4 \in RVVV \subset \mathcal{P}^4$ and start with the projection of $p_4$ to level zero, $\pi_{4,0}(p_4) = p_0$. Since all the points at level zero are equivalent, then one is free to choose any representative for $p_0$. For simplicity, it is easiest to choose it to be the point $p_0 = \mathbf{0}$ and fix coordinates there. Next, we look at all the points at the first level, which project to $p_0$. Since all these points at level 1 are equivalent it means that there is a single orbit in the first level and we are again able to choose any point in $\mathcal{P}^1$ as our representive so long as it projects to the point $p_0$. We will pick $p_1 = (0,0,0,[1:0:0]) = (0,0,0,0,0)$ with $u = \frac{dy}{dx}$ and $v = \frac{dz}{dx}$, and we will look at all the diffeomorphisms $\Phi$ that fix the point $p_0$ and satisfying $\Phi_*([1:0:0]) = [1:0:0]$. Note, by an abuse of notation, that when we write "$\Phi_*([1:0:0]) = [1:0:0]$" we mean the pushforward of $\Phi$, at the point $p_0$, which fixes the line $span\{\frac{\partial}{\partial x}\}$ in $\Delta_0(p_0)$. This condition will place some restrictions on the component functions of the diffeomorphism germs $\Phi$ in $Diff_0(3)$ when we evaluate at the point $p_0$ and tell us what $\Phi^1 = (\Phi, \Phi_*)$ will look like at the point $p_1$. We call this group of diffeomorphisms $G_1$. We can then move on to the second level and look at the class $RV$. Any $p_2 \in RV$ is of the form $p_2 = (p_1, \ell_1)$ with $\ell_1$ contained in the vertical hyperplane inside of $\Delta_1(p_1)$. Now, apply the pushforwards of the $\Phi^1$'s in $G_1$ to the vertical hyperplane and see if these symmetries will act transitively on the critical hyperplane. If they do act transitively then there is a single orbit within the class $RV$. If not, then there exists more than one orbit within the class $RV$. We then count the number of different equivalence classes there are within this hyperplane and that number tells us how many orbits there are within that class. Again, we want to point out that there could be an infinite number of equivalence classes. Note that because of Theorem 3.5, we should expect to only see one orbit within this class. Once this is done, we can just iterate the above process to classify the number of orbits within the class $RVV$ at the third level and then within the class $RVVV$ at the fourth level.

- *Level* 0: Let $G_0$ $(= Diff_0(3))$ be the group of all diffeomorphism germs that fix the origin.
- *Level* 1: We know that all the points in $\mathcal{P}^1$ are equivalent, thus there is only a single orbit. So we pick a representative element from the single orbit of $\mathcal{P}^1$. We will take our representative to be $p_1 = (0,0,0,0,0) = (0,0,0,[1:0:0]) = (x,y,z,[dx:dy:dz])$ and take $G_1$ to be the set of all $\Phi \in G_0$ such that $\Phi^1$ will take the lines tangent to the $x$-axis back to the $x$-axis, meaning $\Phi_*([1:0:0]) = [1:0:0]$.
  Then for $\Phi \in G_1$ and $\Phi(x,y,z) = (\phi^1(x,y,z), \phi^2(x,y,z), \phi^3(x,y,z))$ we must have
$$\Phi_* = \begin{pmatrix} \phi^1_x & \phi^1_y & \phi^1_z \\ \phi^2_x & \phi^2_y & \phi^2_z \\ \phi^3_x & \phi^3_y & \phi^3_z \end{pmatrix} = \begin{pmatrix} \phi^1_x & \phi^1_y & \phi^1_z \\ 0 & \phi^2_y & \phi^2_z \\ 0 & \phi^3_y & \phi^3_z \end{pmatrix}$$
  when we evaluate at $(x,y,z) = (0,0,0)$.
  Here is the *Taylor triangle* representing the different coefficients in the Taylor series of a diffeomorphism in $G_i$. The three digits represent the number of partial derivatives with respect to either $x$, $y$, or $z$. For example, $(1,2,0) = \frac{\partial^3}{\partial x \partial^2 y}$. The vertical column denotes the coefficient order. We start with the Taylor triangle for $\phi^2$:

| | | | | | | |
|---|---|---|---|---|---|---|
| $n=0$: | | | ~~(0, 0, 0)~~ | | | |
| $n=1$: | | ~~(1, 0, 0)~~ | (0, 1, 0) | (0, 0, 1) | | |
| $n=2$: | (2, 0, 0) | (1, 1, 0) | (1, 0, 1) | (0, 2, 0) | (0, 1, 1) | (0, 0, 2) |

  We have crossed out $(1,0,0)$ since $\frac{\partial \phi^2}{\partial x}(\mathbf{0}) = 0$. Next is the Taylor triangle for $\phi^3$:

| | | | | | | |
|---|---|---|---|---|---|---|
| $n=0$: | | | ~~(0, 0, 0)~~ | | | |
| $n=1$: | | ~~(1, 0, 0)~~ | (0, 1, 0) | (0, 0, 1) | | |
| $n=2$: | (2, 0, 0) | (1, 1, 0) | (1, 0, 1) | (0, 2, 0) | (0, 1, 1) | (0, 0, 2) |

  This describes some properties of the elements $\Phi \in G_1$.
  We now try to figure out what $\Phi^1$, for $\Phi \in G_1$, will look like in $KR$-coordinates. First, we look at a line $\ell \subset \Delta_0$ and write $\ell = span\{a\frac{\partial}{\partial x} + b\frac{\partial}{\partial y} + c\frac{\partial}{\partial z}\}$ with $a,b,c \in \mathbb{R}$ and $a \neq 0$.
  Applying the pushforward of $\Phi$ to the line $\ell$ we get
$$\begin{aligned} \Phi_*(\ell) &= span\left\{ \left(a\phi^1_x + b\phi^1_y + c\phi^1_z\right)\frac{\partial}{\partial x} + \left(a\phi^2_x + b\phi^2_y + c\phi^2_z\right)\frac{\partial}{\partial y} + \left(a\phi^3_x + b\phi^3_y + c\phi^3_z\right)\frac{\partial}{\partial z} \right\} \\ &= span\left\{ \left(\phi^1_x + u\phi^1_y + v\phi^1_z\right)\frac{\partial}{\partial x} + \left(\phi^2_x + u\phi^2_y + v\phi^2_z\right)\frac{\partial}{\partial y} + \left(\phi^3_x + u\phi^3_y + v\phi^3_z\right)\frac{\partial}{\partial z} \right\} \\ &= span\left\{ a_1\frac{\partial}{\partial x} + a_2\frac{\partial}{\partial y} + a_3\frac{\partial}{\partial z} \right\} \end{aligned}$$
  where in the second line we divided by $a$ and wrote $u = \frac{b}{a}$ and $v = \frac{c}{a}$. Now, since $\Delta_1$ is given by

$$dy - u\,dx = 0,$$
$$dz - v\,dx = 0.$$

Since $[dx : dy : dz] = [1 : \frac{dy}{dx} : \frac{dz}{dx}]$ we have for $\Phi \in G_1$ we write $\Phi^1$ in local coordinates as $\Phi^1(x, y, z, u, v) = (\phi^1, \phi^2, \phi^3, \tilde{u}, \tilde{v})$ where

$$\tilde{u} = \frac{a_2}{a_1} = \frac{\phi^2_x + u\phi^2_y + v\phi^2_z}{\phi^1_x + u\phi^1_y + v\phi^1_z},$$
$$\tilde{v} = \frac{a_3}{a_1} = \frac{\phi^3_x + u\phi^3_y + v\phi^3_z}{\phi^1_x + u\phi^1_y + v\phi^1_z}.$$

- *Level* 2: At level 2 we are looking at the class $RV$ which consists of a single orbit by Theorem 3.5. This means that we can pick any point in the class $RV$ as our representative. We will pick our point to be $p_2 = (p_1, \ell_1)$ with $\ell_1 \subset \Delta_1(p_1)$ equal to the vertical line $\ell_1 = [dx : du : dv] = [0 : 1 : 0]$. Now, we will let $G_2$ be the set of symmetries from $G_1$ that fix the vertical line $\ell_1 = [0 : 1 : 0]$ in $\Delta_1(p_1)$, those satisfying $\Phi^1_*([0 : 1 : 0]) = [0 : 1 : 0]$ for all $\Phi \in G_2$. This implies $\Phi^1_*([dx|_{\ell_1} : du|_{\ell_1} : dv|_{\ell_1}]) = \Phi^1_*([0 : 1 : 0]) = [0 : 1 : 0] = [d\phi^1|_{\ell_1} : d\tilde{u}|_{|\ell_1} : d\tilde{v}|_{|\ell_1}]$. When we fix this direction it might yield some new information about the component functions of the elements of $G_2$. In particular, we need to set $d\phi^1|_{\ell_1} = 0$ and $d\tilde{v}|_{\ell_1} = 0$.
  - Looking at the restriction $d\phi^1|_{\ell_1} = 0$.
  One has $d\phi^1 = \phi^1_x dx + \phi^1_y dy + \phi^1_z dz$ and when we set $d\phi^1|_{\ell_1} = 0$ we can see that we will not gain any new information about the component functions for $\Phi \in G_2$. This is because the covectors $dx$, $dy$, and $dz$ will be zero along the line $\ell_1$.
  - Looking at the restriction $d\tilde{v}|_{\ell_1} = 0$.
  Can see that $d\tilde{v} = d(\frac{a_3}{a_1}) = \frac{da_3}{a_1} - \frac{(da_1)a_3}{a_1^2}$ and notice when we evaluate at $(x, y, z, u, v) = (0, 0, 0, 0, 0)$, we have $a_3 = 0$, and since we are setting $d\tilde{v}|_{\ell_1} = 0$ then $da_3|_{\ell_1}$ must be equal to zero. We calculate that

$$da_3 = \phi^3_{xx}dx + \phi^3_{xy}dy + \phi^3_{xz}dz + \phi^3_y du + u\big(d\phi^3_y\big) + \phi^3_z dv + v\big(d\phi^3_z\big)$$

and when we evaluate we get

$$da_3|_{\ell_1} = \phi^3_y(\mathbf{0})du|_{\ell_1} = 0.$$

But $du|_{\ell_1} \neq 0$, so $\phi^3_y(\mathbf{0}) = 0$.
This gives us the updated Taylor triangle for $\phi^3$:

| | | | | | | |
|---|---|---|---|---|---|---|
| $n = 0$: | | | ~~(0, 0, 0)~~ | | | |
| $n = 1$: | | ~~(1, 0, 0)~~ | ~~(0, 1, 0)~~ | (0, 0, 1) | | |
| $n = 2$: | (2, 0, 0) | (1, 1, 0) | (1, 0, 1) | (0, 2, 0) | (0, 1, 1) | (0, 0, 2) |

We have determined some of the properties of elements in $G_2$ and now we will see what these elements look like locally. We look at a point $p_1'$ near the point $p_1$ and at $\Phi^1_*(\ell)$ for $\ell \subset \Delta_1(p_1')$, near the vertical hyperplane in $\Delta_1(p_1')$, which is of the form $\ell = span\{aX^{(1)} + b\frac{\partial}{\partial u} + c\frac{\partial}{\partial v}\}$ with $a, b, c \in \mathbb{R}$ and $b \neq 0$ with $X^{(1)} = u\frac{\partial}{\partial y} + v\frac{\partial}{\partial z} + \frac{\partial}{\partial x}$. Let $\mathbf{w} = aX^{(1)} + b\frac{\partial}{\partial u} + c\frac{\partial}{\partial v}$ and we apply $\Phi^1_*$ to $\mathbf{w}$ to get

$$\Phi^1_*(\mathbf{w}) = \begin{pmatrix} \phi^1_x & \phi^1_y & \phi^1_z & 0 & 0 \\ \phi^2_x & \phi^2_y & \phi^2_z & 0 & 0 \\ \phi^3_x & \phi^3_y & \phi^3_z & 0 & 0 \\ \frac{\partial\tilde{u}}{\partial x} & \frac{\partial\tilde{u}}{\partial y} & \frac{\partial\tilde{u}}{\partial z} & \frac{\partial\tilde{u}}{\partial u} & \frac{\partial\tilde{u}}{\partial v} \\ \frac{\partial\tilde{v}}{\partial x} & \frac{\partial\tilde{v}}{\partial y} & \frac{\partial\tilde{v}}{\partial z} & \frac{\partial\tilde{v}}{\partial u} & \frac{\partial\tilde{v}}{\partial v} \end{pmatrix} \begin{pmatrix} a \\ au \\ av \\ b \\ c \end{pmatrix}$$
$$= \big(a\phi^1_x + au\phi^1_y + av\phi^1_z\big)\frac{\partial}{\partial x} + \left(a\frac{\partial\tilde{u}}{\partial x} + au\frac{\partial\tilde{u}}{\partial y} + av\frac{\partial\tilde{u}}{\partial z} + b\frac{\partial\tilde{u}}{\partial u} + c\frac{\partial\tilde{u}}{\partial v}\right)\frac{\partial}{\partial u}$$
$$+ \left(a\frac{\partial\tilde{v}}{\partial x} + au\frac{\partial\tilde{v}}{\partial y} + av\frac{\partial\tilde{v}}{\partial z} + b\frac{\partial\tilde{v}}{\partial u} + c\frac{\partial\tilde{v}}{\partial v}\right)\frac{\partial}{\partial v}.$$

This means that when we look at $\Phi^1_*$ applied to the line $\ell$ we get

$$\Phi^1_*(\ell) = span\left\{\big(a\phi^1_x + au\phi^1_y + av\phi^1_z\big)\frac{\partial}{\partial x} + \left(a\frac{\partial\tilde{u}}{\partial x} + au\frac{\partial\tilde{u}}{\partial y} + av\frac{\partial\tilde{u}}{\partial z} + b\frac{\partial\tilde{u}}{\partial u} + c\frac{\partial\tilde{u}}{\partial v}\right)\frac{\partial}{\partial u}\right.$$

$$
\begin{aligned}
&+\left(a\frac{\partial\tilde{v}}{\partial x}+au\frac{\partial\tilde{v}}{\partial y}+av\frac{\partial\tilde{v}}{\partial z}+b\frac{\partial\tilde{v}}{\partial u}+c\frac{\partial\tilde{v}}{\partial v}\right)\frac{\partial}{\partial v}\Bigg\}\\
&=span\Bigg\{\left(u_2\phi_x^1+uu_2\phi_y^1+vu_2\phi_z^1\right)\frac{\partial}{\partial x}+\left(u_2\frac{\partial\tilde{u}}{\partial x}+uu_2\frac{\partial\tilde{u}}{\partial y}+vu_2\frac{\partial\tilde{u}}{\partial z}+\frac{\partial\tilde{u}}{\partial u}+v_2\frac{\partial\tilde{u}}{\partial v}\right)\frac{\partial}{\partial u}\\
&\quad+\left(u_2\frac{\partial\tilde{v}}{\partial x}+uu_2\frac{\partial\tilde{v}}{\partial y}+vu_2\frac{\partial\tilde{v}}{\partial z}+\frac{\partial\tilde{v}}{\partial u}+v_2\frac{\partial\tilde{v}}{v}\right)\frac{\partial}{\partial v}\Bigg\}\\
&=span\left\{b_1\frac{\partial}{\partial x}+b_2\frac{\partial}{\partial u}+b_3\frac{\partial}{\partial v}\right\}.
\end{aligned}
$$

Notice that we have only paid attention to the $x$, $u$, and $v$ coordinates since $\Delta_1$ is framed by $dx$, $du$, and $dv$. Since $u_2=\frac{dx}{du}$ and $v_2=\frac{dv}{du}$ we get

$$
\begin{aligned}
\tilde{u}_2&=\frac{b_1}{b_2}=\frac{u_2\phi_x^1+uu_2\phi_y^1+vu_2\phi_z^1}{u_2\frac{\partial\tilde{u}}{\partial x}+uu_2\frac{\partial\tilde{u}}{\partial y}+vu_2\frac{\partial\tilde{u}}{\partial z}+\frac{\partial\tilde{u}}{\partial u}+v_2\frac{\partial\tilde{u}}{\partial v}},\\
\tilde{v}_2&=\frac{b_3}{b_2}=\frac{u_2\frac{\partial\tilde{v}}{\partial x}+uu_2\frac{\partial\tilde{v}}{\partial y}+vu_2\frac{\partial\tilde{v}}{\partial z}+\frac{\partial\tilde{v}}{\partial u}+v_2\frac{\partial\tilde{v}}{\partial v}}{u_2\frac{\partial\tilde{u}}{\partial x}+uu_2\frac{\partial\tilde{u}}{\partial y}+vu_2\frac{\partial\tilde{u}}{\partial z}+\frac{\partial\tilde{u}}{\partial u}+v_2\frac{\partial\tilde{u}}{\partial v}}.
\end{aligned}
$$

The above equations now tell us what the new component functions $\tilde{u}_2$ and $\tilde{v}_2$ are for $\Phi^2$ in a neighborhood of $p_2$.

- *Level* 3: At level 3 we are looking at the class $RVV$. We know from our work on the third level that there will be only one orbit within this class. This means that we can pick any point in the class $RVV$ as our representative. We will pick the point $p_3=(p_2,\ell_2)$ with $\ell_2\subset\Delta_2$ equal to the vertical line $\ell_2=[du:du_2:dv_2]=[0:1:0]$. Now, we will let $G_3$ be the set of symmetries from $G_2$ that fix the vertical line $\ell_2=[0:1:0]$ in $\Delta_2$, meaning we want $\Phi_*^2([0:1:0])=[0:1:0]=[d\tilde{u}|_{\ell_3}:d\tilde{u}_2|_{\ell_3}:d\tilde{v}_2|_{\ell_3}]$ for all $\Phi\in G_3$. Since we are taking $du|_{\ell_3}0$ and $dv_2|_{\ell_3}=0$, with $du_2|_{\ell_3}\neq 0$ we need to look at $d\tilde{u}|_{\ell_3}=0$ and $d\tilde{v}_2|_{\ell_3}=0$ to see if these relations will give us more information about the component functions of $\Phi$.
  - Looking at the restriction $d\tilde{u}|_{\ell_3}=0$.

  Looking at $d\tilde{u}=d(\frac{a_2}{a_1})=\frac{da_2}{a_1}-\frac{a_2da_1}{a_1^2}$ and since $a_2(p_2)=0$, we must have $da_2|_{\ell_3}=0$. When we evaluate this expression one finds $da_2|_{\ell_3}=\phi_{xx}^2dx|_{\ell_3}+\phi_{xy}^2dy|_{\ell_3}+\phi_{xz}^2dz|_{\ell_3}+\phi_y^2du|_{\ell_3}+\phi_z^2dv|_{\ell_3}=0$. Since all the differentials are going to be equal to zero when we evaluate them along the line $\ell_3$ then we do not gain any new information about the $\phi^i$'s.
  - Looking at the restriction $d\tilde{v}_2|_{\ell_3}=0$.

  $d\tilde{v}_2=d(\frac{b_3}{b_2})=\frac{db_3}{b_2}-\frac{b_3db_2}{b_2^2}$. Evaluating we find $b_3(p_2)=0$ since $\frac{\partial\tilde{v}}{\partial u}(p_2)=\phi_y^3(\mathbf{0})=0$, which implies that we only need to look at $\frac{db_3}{b_2}$. We compute

$$
\begin{aligned}
db_3&=d\left(u_2\frac{\partial\tilde{v}}{\partial x}+u_2u\frac{\partial\tilde{v}}{\partial z}+\frac{\partial\tilde{v}}{\partial u}+v_2\frac{\partial\tilde{v}}{\partial v}\right)\\
&=\frac{\partial\tilde{v}}{\partial x}du_2+u_2\left(d\frac{\partial\tilde{v}}{\partial x}\right)+u\frac{\partial\tilde{v}}{\partial y}du_2+u_2\frac{\partial\tilde{v}}{\partial y}du+u_2u\left(d\frac{\partial\tilde{v}}{\partial y}\right)+v\frac{\partial\tilde{v}}{\partial z}du_2\\
&\quad+u_2\frac{\partial\tilde{v}}{\partial z}dv+u_2v\left(d\frac{\partial\tilde{v}}{\partial z}\right)+\frac{\partial\tilde{v}}{\partial u\partial x}dx+\frac{\partial\tilde{v}}{\partial u\partial y}dy+\frac{\partial\tilde{u}}{\partial u\partial z}dz+\frac{\partial\tilde{v}}{\partial v}dv_2+v_2\left(d\frac{\partial\tilde{v}}{\partial v}\right).
\end{aligned}
$$

Evaluating we get $db_3|_{\ell_3}=\frac{\partial\tilde{v}}{\partial x}(p_3)du_2|_{\ell_3}=0$, and since $du_2|_{\ell_3}\neq 0$ this forces $\frac{\partial\tilde{v}}{\partial x}(p_3)=0$. We have $\frac{\partial\tilde{v}}{\partial x}(p_3)=\frac{\phi_{xx}^3(\mathbf{0})}{\phi_x^1(\mathbf{0})}-\frac{\phi_{xx}^1(\mathbf{0})\phi_x^3(\mathbf{0})}{\phi_x^1(\mathbf{0})}$ and $\phi_x^3(\mathbf{0})=0$, which give $\frac{\partial\tilde{v}}{\partial x}(p_3)=\frac{\phi_{xx}^3(\mathbf{0})}{\phi_x^1(\mathbf{0})}=0$ which forces $\phi_{xx}^3(\mathbf{0})=0$. This gives us information about $\Phi^3$ along with the updated Taylor triangle for $\phi^3$:

$$
\begin{array}{lccccccc}
n=0: & & & \cancel{(0,0,0)} & & & & \\
n=1: & & \cancel{(1,0,0)} & \cancel{(0,1,0)} & (0,0,1) & & & \\
n=2: & \cancel{(2,0,0)} & (1,1,0) & (1,0,1) & (0,2,0) & (0,1,1) & (0,0,2) &
\end{array}
$$

Now, our goal is to look at how the $\Phi_*^3$'s act on the distribution $\Delta_3(p_3)$ in order to determine the number of orbits within the class $RVVV$. In order to do so we will need to figure out what the local component functions, call them $\tilde{u}_3$ and $\tilde{v}_3$, are for $\Phi^3$, with $\Phi\in G_3$. To do this we will again look at $\Phi_*^2$ applied to a line $\ell$ that is near the vertical hyperplane in $\Delta_2$.

Set $\ell = span\{aX^{(2)} + b\frac{\partial}{\partial u_2} + c\frac{\partial}{\partial v_2}\}$ for $a, b, c \in \mathbb{R}$ and $b \neq 0$ where $X^{(2)} = u_2(u\frac{\partial}{\partial y} + v\frac{\partial}{\partial z} + \frac{\partial}{\partial x}) + \frac{\partial}{\partial u} + v_2\frac{\partial}{\partial v}$. Let $\mathbf{w} = aX^{(2)} + b\frac{\partial}{\partial u_2} + c\frac{\partial}{\partial v_2}$ and we compute

$$\Phi^2_*(\mathbf{w}) = \begin{pmatrix} \phi^1_x & \phi^1_y & \phi^1_z & 0 & 0 & 0 & 0 \\ \phi^2_x & \phi^2_y & \phi^2_z & 0 & 0 & 0 & 0 \\ \phi^3_x & \phi^3_y & \phi^3_z & 0 & 0 & 0 & 0 \\ \frac{\partial\tilde{u}}{\partial x} & \frac{\partial\tilde{u}}{\partial y} & \frac{\partial\tilde{u}}{\partial z} & \frac{\partial\tilde{u}}{\partial u} & \frac{\partial\tilde{u}}{\partial v} & 0 & 0 \\ \frac{\partial\tilde{v}}{\partial x} & \frac{\partial\tilde{v}}{\partial y} & \frac{\partial\tilde{v}}{\partial z} & \frac{\partial\tilde{v}}{\partial u} & \frac{\partial\tilde{v}}{\partial v} & 0 & 0 \\ \frac{\partial\tilde{u}_2}{\partial x} & \frac{\partial\tilde{u}_2}{\partial y} & \frac{\partial\tilde{u}_2}{\partial z} & \frac{\partial\tilde{u}_2}{\partial u} & \frac{\partial\tilde{u}_2}{\partial v} & \frac{\partial\tilde{u}_2}{\partial u_2} & \frac{\partial\tilde{u}_2}{\partial v_2} \\ \frac{\partial\tilde{v}_2}{\partial x} & \frac{\partial\tilde{v}_2}{\partial y} & \frac{\partial\tilde{v}_2}{\partial z} & \frac{\partial\tilde{v}_2}{\partial u} & \frac{\partial\tilde{v}_2}{\partial v} & \frac{\partial\tilde{v}_2}{\partial u_2} & \frac{\partial\tilde{v}_2}{\partial v_2} \end{pmatrix} \begin{pmatrix} au_2 \\ auu_2 \\ avu_2 \\ a \\ av_2 \\ b \\ c \end{pmatrix}.$$

Then for $\Phi^2_*$ applied to the line $\ell$ we end up with it being equal to

$$\begin{aligned} &span\left\{\left(au_2\frac{\partial\tilde{u}}{\partial x} + auu_2\frac{\partial\tilde{u}}{\partial y} + avu_2\frac{\partial\tilde{u}}{\partial z} + a\frac{\partial\tilde{u}}{\partial u} + av_2\frac{\partial\tilde{u}}{\partial v}\right)\frac{\partial}{\partial u}\right. \\ &\quad + \left(au_2\frac{\partial\tilde{u}_2}{\partial x} + auu_2\frac{\partial\tilde{u}_2}{\partial y} + avu_2\frac{\partial\tilde{u}_2}{\partial z} + a\frac{\partial\tilde{u}_2}{\partial u} + av_2\frac{\partial\tilde{u}_2}{\partial v} + b\frac{\partial\tilde{u}_2}{\partial u_2} + c\frac{\partial\tilde{u}_2}{\partial v_2}\right)\frac{\partial}{\partial u_2} \\ &\quad \left. + \left(au_2\frac{\partial\tilde{v}_2}{\partial x} + auu_2\frac{\partial\tilde{v}_2}{\partial y} + avu_2\frac{\partial\tilde{v}_2}{\partial z} + a\frac{\partial\tilde{v}_2}{\partial u} + av_2\frac{\partial\tilde{v}_2}{\partial v} + b\frac{\partial\tilde{v}_2}{\partial u_2} + c\frac{\partial\tilde{v}_2}{\partial v_2}\right)\frac{\partial}{\partial v_2}\right\} \\ &= span\left\{\left(u_3u_2\frac{\partial\tilde{u}}{\partial x} + u_3uu_2\frac{\partial\tilde{u}}{\partial y} + u_3vu_2\frac{\partial\tilde{u}}{\partial z} + u_3\frac{\partial\tilde{u}}{\partial u} + u_3v_2\frac{\partial\tilde{u}}{\partial v}\right)\frac{\partial}{\partial u}\right. \\ &\quad + \left(u_3u_2\frac{\partial\tilde{u}_2}{\partial x} + u_3uu_2\frac{\partial\tilde{u}_2}{\partial y} + u_3vu_2\frac{\partial\tilde{u}_2}{\partial z} + u_3\frac{\partial\tilde{u}_2}{\partial u} + u_3v_2\frac{\partial\tilde{u}_2}{\partial v} + \frac{\partial\tilde{u}_2}{\partial u_2} + v_3\frac{\partial\tilde{u}_2}{\partial v_2}\right)\frac{\partial}{\partial u_2} \\ &\quad \left. + \left(u_3u_2\frac{\partial\tilde{v}_2}{\partial x} + u_3uu_2\frac{\partial\tilde{v}_2}{\partial y} + u_3vu_2\frac{\partial\tilde{v}_2}{\partial z} + u_3\frac{\partial\tilde{v}_2}{\partial u} + u_3v_2\frac{\partial\tilde{v}_2}{\partial v} + \frac{\partial\tilde{v}_2}{\partial u_2} + v_3\frac{\partial\tilde{v}_2}{\partial v_2}\right)\frac{\partial}{\partial v_2}\right\} \\ &= span\left\{c_1\frac{\partial}{\partial u} + c_2\frac{\partial}{\partial u_2} + c_3\frac{\partial}{\partial v_2}\right\}, \end{aligned}$$

because our local coordinates are given by $[du : du_2 : dv_2] = [\frac{du}{du_2} : 1 : \frac{dv_2}{du_2}] = [u_3 : 1 : v_3]$ we end up with

$$\tilde{u}_3 = \frac{c_1}{c_2} = \frac{u_3u_2\frac{\partial\tilde{u}}{\partial x} + u_3uu_2\frac{\partial\tilde{u}}{\partial y} + u_3vu_2\frac{\partial\tilde{u}}{\partial z} + u_3\frac{\partial\tilde{u}}{\partial u} + u_3v_2\frac{\partial\tilde{u}}{\partial v}}{u_3u_2\frac{\partial\tilde{u}_2}{\partial x} + u_3uu_2\frac{\partial\tilde{u}_2}{\partial y} + u_3vu_2\frac{\partial\tilde{u}_2}{\partial z} + u_3\frac{\partial\tilde{u}_2}{\partial u} + u_3v_2\frac{\partial\tilde{u}_2}{\partial v} + \frac{\partial\tilde{u}_2}{\partial u_2} + v_3\frac{\partial\tilde{u}_2}{\partial v_2}},$$

$$\tilde{v}_3 = \frac{c_3}{c_2} = \frac{u_3u_2\frac{\partial\tilde{v}_2}{\partial x} + u_3uu_2\frac{\partial\tilde{v}_2}{\partial y} + u_3vu_2\frac{\partial\tilde{v}_2}{\partial z} + u_3\frac{\partial\tilde{v}_2}{\partial u} + u_3v_2\frac{\partial\tilde{v}_2}{\partial v} + \frac{\partial\tilde{v}_2}{\partial u_2} + v_3\frac{\partial\tilde{v}_2}{\partial v_2}}{u_3u_2\frac{\partial\tilde{u}_2}{\partial x} + u_3uu_2\frac{\partial\tilde{u}_2}{\partial y} + u_3vu_2\frac{\partial\tilde{u}_2}{\partial z} + u_3\frac{\partial\tilde{u}_2}{\partial u} + u_3v_2\frac{\partial\tilde{u}_2}{\partial v} + \frac{\partial\tilde{u}_2}{\partial u_2} + v_3\frac{\partial\tilde{u}_2}{\partial v_2}}.$$

- *Level* 4: Now that we know what the component functions are for $\Phi^3$, with $\Phi \in G_3$, we are ready to apply its pushforward to the distribution $\Delta_3$ at $p_3$ and figure out how many orbits there are for the class $RVVV$. We let $\ell = span\{b\frac{\partial}{\partial u_3} + c\frac{\partial}{\partial v_3}\}$, with $b, c \in \mathbb{R}$ and $b \neq 0$, be a vector in the vertical hyperplane of $\Delta_3(p_3)$ and we see that

$$\Phi^3_*(\ell) = span\left\{\left(b\frac{\partial\tilde{u}_3}{\partial u_3}(p_3) + c\frac{\partial\tilde{u}_3}{\partial v_3}(p_3)\right)\frac{\partial}{\partial u_3} + \left(b\frac{\partial\tilde{v}_3}{\partial u_3}(p_3) + c\frac{\partial\tilde{v}_3}{\partial v_3}(p_3)\right)\frac{\partial}{\partial v_3}\right\}.$$

This means that we need to compute $\frac{\partial\tilde{u}_3}{\partial u_3}(p_3)$, $\frac{\partial\tilde{u}_3}{\partial v_3}(p_3)$, $\frac{\partial\tilde{v}_3}{\partial u_3}(p_3)$, and $\frac{\partial\tilde{v}_3}{\partial v_3}(p_3)$ where $p_3 = (x, y, z, u, v, u_2, v_2, u_3, v_3) = (0, 0, 0, 0, 0, 0, 0, 0, 0)$. This will amount to a somewhat long process, so we will just state what the above terms are equal to *and leave the computations for Appendix A*. After evaluating we will see that $\Phi^3_*(\ell) = span\{(b\frac{(\phi^2_y(\mathbf{0}))^2}{(\phi^1_x(\mathbf{0}))^3})\frac{\partial}{\partial u_3} + (c\frac{\phi^3_z(\mathbf{0})}{(\phi^1_x(\mathbf{0}))^2})\frac{\partial}{\partial v_3}\}$. This means that for $\ell = span\{\frac{\partial}{\partial u_3}\}$ $(c = 0)$ we get $\Phi^3_*(\ell) = span\{\frac{(\phi^2_y(\mathbf{0}))^2}{(\phi^1_x(\mathbf{0}))^3}\frac{\partial}{\partial u_3}\}$ to give one orbit. This orbit is characterized by all vectors of the form $b'\frac{\partial}{\partial u_3}$ with $b' \neq 0$. Then, for $\ell = span\{\frac{\partial}{\partial u_3} + \frac{\partial}{\partial v_3}\}$ we see that $\Phi^3_*(\ell) = span\{(\frac{(\phi^2_y(\mathbf{0}))^2}{(\phi^1_x(\mathbf{0}))^3})\frac{\partial}{\partial u_3} + (\frac{\phi^3_z(\mathbf{0})}{(\phi^1_x(\mathbf{0}))^2})\frac{\partial}{\partial v_3}\}$, and notice that $\phi^1_x(\mathbf{0}) \neq 0$, $\phi^2_y(\mathbf{0}) \neq 0$, and $\phi^3_z(\mathbf{0}) \neq 0$. However, we can choose

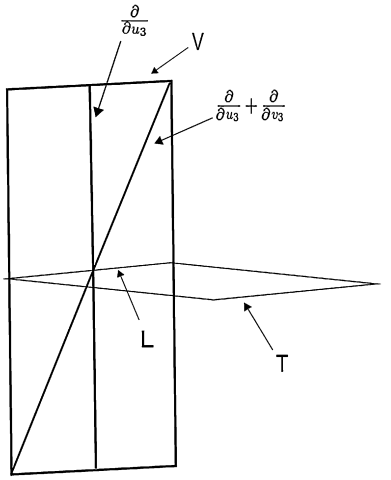


**Fig. 4.** Orbits within the class $RVVV$.

$\phi_x^1(\mathbf{0})$, $\phi_y^2(\mathbf{0})$, and $\phi_z^3(\mathbf{0})$ to be equal to anything else other than zero. Then since our distribution $\Delta_3(p_3)$ is coframed by $du_2, du_3, dv_3$ and with $\ell' \equiv \Phi_*^3(\ell)$ we get

$$\left[du_2|_{\ell'}, du_3|_{\ell'}, dv_3|_{\ell'}\right] = \left[0, \frac{(\phi_y^2(\mathbf{0}))^2}{(\phi_x^1(\mathbf{0}))^3}, \frac{\phi_z^3(\mathbf{0})}{(\phi_x^1(\mathbf{0}))^2}\right] = \left[0, 1, \frac{\phi_x^1(\mathbf{0})\phi_z^3(\mathbf{0})}{(\phi_y^2(\mathbf{0}))^2}\right]$$

to give another, separate orbit. In the present case, for $\ell$ to be a vertical direction, it must be of the form $\ell = span\{b\frac{\partial}{\partial u_3} + c\frac{\partial}{\partial v_3}\}$ with $b \neq 0$. This means that there is a total of 2 orbits for the class $RVVV$, as depicted in Fig. 4.

The classification of the other $RVT$ classes at level 4 are done in a very similar manner. The details of these other calculations will be given in a subsequent work by one of the authors.

## 6. Conclusion

We have exhibited a canonical procedure for lifting the action of $Diff(3)$ to the fibered manifold $\mathcal{P}^k(2)$, and by a mix of singularity theory of space curves and the representation theory of diffeomorphism groups we were able to completely classify orbits of this extended action for small values of $k$. A cursory glance at our computational methods will convince the reader that these results can nominally be extended to higher values of $k$, but with an exponential increase in computational effort. Progress has been made to try and extend the classification results of the present paper and we hope to release these findings sometime in the near future. In [6] we already called the attention to a lack of discrete invariants to assist with the *full classification problem*. Most combinatorial invariants for analytic space curves are inequivalent [5], and it remains to find out if our $RVT$ coding is equivalent to any/some of them. *Can one use these invariants to simplify the classification task?* Let us remind the reader that when $n = 1$ the fortuitous coincidence that all discrete invariants of planar curves provide essentially the same combinatorial information helped reduce the classification effort considerably.

When we originally posted our paper in July of 2011 we had made a conjecture concerning a recent paper by Li and Respondek. In [13], Li and Respondek constructed a mechanical system consisting of $k$-rigid bars moving in $\mathbb{R}^{n+1}$ subject to a nonholonomic constraint which is equivalent to the Cartan distribution of $J^k(\mathbb{R}, \mathbb{R}^n)$ at regular configuration points. We originally conjectured that the singular configurations of the $k$-bar would be related or have some connection to singular Goursat multi-flags similar to those presented here, though in Li and Respondek's case the configuration manifold is a tower of $S^n$ fibrations instead of our $\mathbb{P}^n$ tower. As of November 2011, F. Pelletier [21] was able to exhibit this *concrete relationship* that we were searching for. Pelletier defined the notion of Cartan spherical prolongation which gives rise to a tower of sphere bundles, similar to how Cartan projective prolongations gives us the Monster Tower. As a corollary of his construction each level of his spherical Monster Tower provides us with a canonical 2-fold covering of each corresponding level of the projective Monster Tower.

Another research venue, which to our knowledge has been little explored, is looking at how these results could be applied to the geometric theory of differential equations. Let us remind the reader that the spaces $\mathcal{P}^k(2)$, or more generally $\mathcal{P}^k(n)$ are fiber compactifications of the jet spaces $J^k(\mathbb{R}, \mathbb{R}^2)$ and $J^k(\mathbb{R}, \mathbb{R}^n)$ respectively. Intuitively one may think that derivatives are allowed to blow-up in this new theory. Kumpera and Rubin [12] have used the geometric theory to study underdetermined systems of ordinary differential equations (e.g. control systems), but it remains to be explored how our classification results, and compactification procedures can provide new qualitative information concerning overdetermined systems of differential equations.

**Acknowledgements**

We would like to warmly thank Corey Shanbrom (UCSC) for a very thorough revision of an early version of this manuscript, and Richard Montgomery (UCSC) for many useful conversations and remarks. A.C. also thanks Susan Colley (Oberlin) and Gary Kennedy (UO) for suggesting to us the Taylor triangle as a bookkeeping device for dealing with isotropy representations. We both thank the referee whose comments helped to improve the overall clarity of the text.

## Appendix A

### A.1. Definition of a Goursat n-flag

In this section we present the definition of a Goursat $n$-flag of length $k$, or what is also referred to as a Special $n$-flag of length $k$. We follow the definition presented in [22].

Let $n \geqslant 2$, $k$ be a non-negative integer and $D$ be a distribution of rank $n+1$. Assume further that the ambient manifold $Z$ has dimension $(n+1)+kn$.

Our distribution $D$ will be defined locally by the vanishing of the one forms $\omega_i$ for $i = 1, \ldots, s$, which are pointwise linearly independent as covectors.

The *Cauchy characteristic system* of $D$ is the linear subbundle defined by the linear constraints

$$Ch(D)(p) = \left\{ X \in D(p) \;\middle|\; X \lrcorner d\omega_i = 0 \bmod \omega_i,\ \forall i \in \{1, \ldots, s\} \right\}.$$

We say that a nonholonomic distribution $D$ admits a *special $n$-flag of length $k$* if it has integrable subbundle $F$ of $\partial^{k-1}D$ of corank 1 and that satisfies the following sandwich diagram:

$$\begin{array}{ccccccccccc} & & D & \subset & \partial D & \cdots \subset & \partial^{k-2}D & \subset & \partial^{k-1}D & \subset & \partial^k D = TZ \\ & & \cup & & \cup & & \cup & & \cup & & \\ Ch(D) & \subset & Ch(\partial D) & \subset & Ch(\partial^2 D) & \cdots \subset & Ch(\partial^{k-1}D) & \subset & F & & \end{array}$$

where $\partial D$ is called the *derived system of $D$*, and geometrically $\partial D = D + [D, D]$. Proceeding recursively, $\partial^i D = \partial(\partial^{i-1}D)$ and we can verify that $\operatorname{rank}(\partial^i D) = \operatorname{rank}(\partial^{i-1}D) + n$ for $i = 1, \ldots, k$. In our language, $F = \ker(d\pi_{k,0})$ for $\pi_{k,0} : \mathcal{P}^k \to \mathbb{R}^3$ [22].

### A.2. A technique to eliminate terms in the short parameterization of a curve germ

The following technique that we will discuss is outlined in [24] on p. 23. Let $C$ be a planar curve germ. A *short parametrization* of $C$ is a parametrization of the form

$$C = \begin{cases} \tilde{x} = t^n, \\ \tilde{y} = t^m + \Sigma_{i=1}^{q} a'_{\nu_i} t^{\nu_i} \end{cases}$$

where the $\nu_1 < \nu_2 < \cdots < \nu_q$ are integers that belong to the set $\{m+1, \ldots, c\}$ which do not belong to the semigroup of the curve $C$. In [24] there is a result, Proposition 2.1, which says that if $C$ is any planar analytic curve germ, then there exists a branch $\tilde{C}$ with the above short parametrization and $\tilde{C}$ is $RL$ equivalent to $C$.

We look at a particular case of the short parametrization where we define $\rho$ to be an integer, less than or equal to $q+1$, and $a_{\nu_i} = 0$ for $i < \rho$, and $a_{\nu_\rho} = b$. This gives a short parametrization of the following form

$$C = \begin{cases} x = t^n, \\ y = t^m + bt^{\nu_\rho} + \Sigma_{i=\rho+1}^{q} a_{\nu_i} t^{\nu_i}, \quad b \neq 0 \text{ if } \rho \neq q+1. \end{cases}$$

Suppose that $\nu_\rho + n \in n\mathbb{Z}_+ + m\mathbb{Z}_+$. Now, notice that $\nu_\rho + n \in m\mathbb{Z}_+$ because $\nu_\rho$ is not in the semigroup of $C$. Let $j \in \mathbb{Z}_+$ be such that $\nu_\rho + n = (j+1)m$; notice that $j \geqslant 1$ since $\nu_\rho > m$. Then set $a = \frac{bn}{m}$ and $x' = t^n + at^{jm} + (\text{terms of degree} > jm)$. Let $\tau^n = t^n + at^{jm} + (\text{terms of degree} > jm)$. From this expression one can show that $t = \tau - \frac{a}{n}\tau^{jm-n+1} + (\text{terms of degree} > jm - n + 1)$, and when we substitute this into the original expression above for $C$ that

$$C = \begin{cases} x' = \tau^n, \\ y = \tau^m + (\text{terms of degree} > \nu_\rho). \end{cases}$$

We can now apply Proposition 2.1 to the above expression for $C$ and see that $C$ admits the parametrization

$$C = \begin{cases} x' = \tau^n, \\ y' = \tau^m + \Sigma_{i=\rho+1}^{q} a'_{\nu_i} \tau^{\nu_i}. \end{cases}$$

We can now apply the above technique to the two curves $(t^3, t^5 + t^7, 0)$ and $(t^3, t^5 - t^7, 0)$ in order to eliminate the $t^7$ in both of these curve germs. This means that these two curves will end up being equivalent to the curve $(t^3, t^5, 0)$.

### A.3. Computations for the class $RVVV$

In this section we work out the computations for the functions $\frac{\partial \tilde{u}_3}{\partial u_3}$, $\frac{\partial \tilde{u}_3}{\partial v_3}$, $\frac{\partial \tilde{v}_3}{\partial u_3}$, $\frac{\partial \tilde{v}_3}{\partial v_3}$ evaluated at $p_3 = (x, y, z, u, v, u_2, v_2, u_3, v_3) = (0, 0, 0, 0, 0, 0, 0, 0, 0)$, which we omitted in Section 5.

(1) Computation of $\frac{\partial \tilde{u}_3}{\partial u_3}$.
Starting with $\tilde{u}_3 = \frac{c_1}{c_2}$, one computes

$$\frac{\partial \tilde{u}_3}{\partial u_3} = \frac{u_2 \frac{\partial \tilde{u}}{\partial x} + u u_2 \frac{\partial \tilde{u}}{\partial y} + \frac{\partial \tilde{u}}{\partial u} + v_2 \frac{\partial \tilde{u}}{\partial v}}{c_2} - \frac{\frac{\partial c_2}{\partial u_3} c_1}{c_2^2}$$

and

$$\frac{\partial \tilde{u}_3}{\partial u_3}(p_3) = \frac{\frac{\partial \tilde{u}}{\partial u}(p_3)}{\frac{\partial \tilde{u}_2}{\partial u_2}(p_3)},$$

since $c_1(p_3) = 0$. We recall that $\frac{\partial \tilde{u}}{\partial u}(p_3) = \frac{\phi_y^2(\mathbf{0})}{\phi_x^1(\mathbf{0})}$, $\frac{\partial \tilde{u}_2}{\partial u_2}(p_3) = \frac{\phi_x^1(\mathbf{0})}{\frac{\partial \tilde{u}}{\partial u}(p_3)}$ to give

$$\frac{\partial \tilde{u}_3}{\partial u_3}(p_3) = \frac{(\phi_y^2(\mathbf{0}))^2}{(\phi_x^1(\mathbf{0}))^3}.$$

(2) Computation of $\frac{\partial \tilde{u}_3}{\partial v_3}$.
Since $\tilde{u}_3 = \frac{c_1}{c_2}$, then

$$\frac{\partial \tilde{u}_3}{\partial v_3}(p_3) = \frac{\frac{\partial c_1}{\partial v_3}(p_3)}{c_2(p_3)} - \frac{\frac{\partial c_2}{\partial v_3}(p_3) c_1(p_3)}{c_2^2(p_3)} = 0,$$

because $c_1$ is not a function of $v_3$ and $c_1(p_3) = 0$.

(3) Computation of $\frac{\partial \tilde{v}_3}{\partial u_3}$.
Have that $\tilde{v}_3 = \frac{c_3}{c_2}$, then

$$\frac{\partial \tilde{v}_3}{\partial u_3} = \frac{u_2 \frac{\partial \tilde{v}_2}{\partial x} + \cdots + \frac{\partial \tilde{v}_2}{\partial u} + v_2 \frac{\partial \tilde{v}_2}{\partial v}}{c_2} - \frac{(u_2 \frac{\partial \tilde{u}_2}{\partial x} + \cdots + \frac{\partial \tilde{u}_2}{\partial u} + \cdots + v_2 \frac{\partial \tilde{u}_2}{\partial v}) c_1}{c_2^2},$$

$$\frac{\partial \tilde{v}_3}{\partial u_3}(p_3) = \frac{\frac{\partial \tilde{v}_2}{\partial u}(p_3)}{\frac{\partial \tilde{u}_2}{\partial u_2}(p_3)} - \frac{\frac{\partial \tilde{u}_2}{\partial u}(p_3) \frac{\partial \tilde{v}_2}{\partial u_2}(p_3)}{(\frac{\partial \tilde{u}_2}{\partial u_2}(p_3))^2}.$$

We will need to figure out what $\frac{\partial \tilde{u}_2}{\partial u_2}$, $\frac{\partial \tilde{v}_2}{\partial u_2}$, and $\frac{\partial \tilde{v}_2}{\partial u}$ are when we evaluate at $p_3$.

(a) $\frac{\partial \tilde{v}_2}{\partial u_2}$.
Recall from work at level 3 that

$$\frac{\partial \tilde{v}_2}{\partial u_2}(p_3) = \frac{\frac{\partial \tilde{v}}{\partial x}(p_3)}{\frac{\partial \tilde{u}}{\partial u}(p_3)} = 0$$

since $\frac{\partial \tilde{v}}{\partial x}(p_3) = \frac{\phi_{xx}^3(\mathbf{0})}{\phi_x^1(\mathbf{0})}$ and have $\phi_{xx}^1(\mathbf{0}) = 0$ to give us $\frac{\partial \tilde{v}_2}{\partial u_2}(p_3) = 0$.
This gives the reduced expression

$$\frac{\partial \tilde{v}_3}{\partial u_3}(p_3) = \frac{\frac{\partial \tilde{v}_2}{\partial u}(p_3)}{\frac{\partial \tilde{u}_2}{\partial u_2}(p_3)}.$$

(b) $\frac{\partial \tilde{v}_2}{\partial u}$.
Recall that $\tilde{v}_2 = \frac{b_3}{b_2}$, then we find

$$\frac{\partial \tilde{v}_2}{\partial u} = \frac{u_2 \frac{\partial^2 \tilde{v}}{\partial x \partial u} + u_2 \frac{\partial \tilde{v}}{\partial y} + \cdots + \frac{\partial \tilde{v}}{\partial^2 u} + v_2 \frac{\partial^2 \tilde{v}}{\partial v \partial u}}{b_2} - \frac{(u_2 \frac{\partial^2 \tilde{u}}{\partial x \partial u} + \cdots + \frac{\partial^2 \tilde{u}}{\partial^2 u} + v_2 \frac{\partial^2 \tilde{u}}{\partial v \partial u}) b_3}{b_2^2},$$

$$\frac{\partial^2 \tilde{v}_2}{\partial u}(p_3) = \frac{\frac{\partial^2 \tilde{v}}{\partial^2 u}(p_3)}{\frac{\partial \tilde{u}}{\partial u}(p_3)} - \frac{\frac{\partial^2 \tilde{u}}{\partial^2 u}(p_3) \frac{\partial \tilde{v}}{\partial u}(p_3)}{(\frac{\partial \tilde{u}}{\partial u}(p_3))^2}$$

since $b_2(p_3) = \frac{\partial \tilde{u}}{\partial u}(p_3)$ and $b_3(p_3) = \frac{\partial \tilde{v}}{\partial u}(p_3)$. In order to find $\frac{\partial \tilde{v}_2}{\partial u}(p_3)$ we will need to determine $\frac{\partial \tilde{v}}{\partial u}(p_3)$, $\frac{\partial^2 \tilde{v}}{\partial^2 u}(p_3)$, and $\frac{\partial^2 \tilde{u}}{\partial^2 u}(p_3)$.

(c) $\frac{\partial \tilde{v}}{\partial u}$.

Recall that $\tilde{v} = \frac{a_3}{a_1}$ and that $\frac{\partial \tilde{v}}{\partial u} = \frac{\phi_y^3}{a_1} - \frac{\phi_y^1 a_3}{a_1^2}$, then

$$\frac{\partial \tilde{v}}{\partial u}(p_3) = \frac{\phi_y^3(\mathbf{0})}{\phi_x^1(\mathbf{0})} - \frac{\phi_y^1(\mathbf{0})\phi_x^3(\mathbf{0})}{(\phi_x^1(\mathbf{0}))^2} = 0$$

since $\phi_y^3(\mathbf{0}) = 0$ and $\phi_x^3(\mathbf{0}) = 0$.

(d) $\frac{\partial^2 \tilde{v}}{\partial^2 u}$.

From the above we have $\frac{\partial \tilde{v}}{\partial u} = \frac{\phi_y^3}{a_1} - \frac{\phi_y^1 a_3}{a_1^2}$, then

$$\frac{\partial^2 \tilde{v}}{\partial^2 u}(p_3) = \frac{0}{a_1(p_3)} - \frac{\phi_y^3(\mathbf{0})\phi_y^1(\mathbf{0})}{a_1^2(p_3)} - \frac{\phi_y^1(\mathbf{0})\phi_y^3(\mathbf{0})}{a_1^2(p_3)} + \frac{(\phi_y^1(\mathbf{0}))^2\phi_x^3(\mathbf{0})}{a_1^3(p_3)} = 0$$

since $\phi_y^3(\mathbf{0}) = 0$ and $\phi_x^3(\mathbf{0}) = 0$.

We do not need to determine what $\frac{\partial^2 \tilde{u}}{\partial^2 u}(p_4)$ is, since $\frac{\partial \tilde{v}}{\partial u}$ and $\frac{\partial^2 \tilde{v}}{\partial^2 u}$ will be zero at $p_3$ and give $\frac{\partial \tilde{v}_3}{\partial u_3}(p_3) = 0$.

(4) Computation of $\frac{\partial \tilde{v}_3}{\partial v_3}$.

Recall that $\tilde{v}_3 = \frac{c_3}{c_2}$, then

$$\frac{\partial \tilde{v}_3}{\partial v_3} = \frac{\frac{\partial \tilde{v}_2}{\partial v_2}}{c_2} - \frac{\frac{\partial \tilde{u}_2}{\partial v_2} c_3}{c_2^2},$$

$$\frac{\partial \tilde{v}_3}{\partial v_3}(p_3) = \frac{\frac{\partial \tilde{v}_2}{\partial v_2}(p_3)}{\frac{\partial \tilde{u}_2}{\partial u_2}(p_3)} - \frac{\frac{\partial \tilde{u}_2}{\partial v_2}(p_3)\frac{\partial \tilde{v}_2}{\partial u_2}(p_3)}{(\frac{\partial \tilde{u}_2}{\partial u_2}(p_3))^2}.$$

This means we need to look at $\frac{\partial \tilde{v}_2}{\partial v_2}$, $\frac{\partial \tilde{u}_2}{\partial v_2}$, $\frac{\partial \tilde{v}_2}{\partial u_2}$, and $\frac{\partial \tilde{u}_2}{\partial u_2}$ evaluated at $p_3$.

(a) $\frac{\partial \tilde{v}_2}{\partial v_2}$.

We recall from an earlier calculation that

$$\frac{\partial \tilde{v}_2}{\partial v_2}(p_3) = \frac{\frac{\partial \tilde{v}}{\partial v}(p_3)}{\frac{\partial \tilde{u}}{\partial u}(p_3)} = \frac{\phi_z^3(\mathbf{0})}{\phi_y^2(\mathbf{0})}.$$

(b) $\frac{\partial \tilde{u}_2}{\partial v_2}$.

It is not hard to see that $\frac{\partial \tilde{u}_2}{\partial v_2}(p_3) = 0$.

(c) $\frac{\partial \tilde{u}_2}{\partial u_2}$.

Recall $\tilde{u}_2 = \frac{b_1}{b_2}$ and that

$$\frac{\partial \tilde{u}_2}{\partial u_2} = \frac{\phi_x^1 + u\phi_y^1 + v\phi_z^1}{b_2} - \frac{(\frac{\partial \tilde{u}}{\partial x} + u\frac{\partial \tilde{u}}{\partial y} + v\frac{\partial \tilde{u}}{\partial z})b_1}{b_2^2},$$

then

$$\frac{\partial \tilde{u}_2}{\partial u_2}(p_3) = \frac{\phi_x^1(\mathbf{0})}{\frac{\partial \tilde{u}}{\partial u}(p_3)} = \frac{(\phi_x^1(\mathbf{0}))^2}{\phi_y^2(\mathbf{0})}.$$

With the above in mind we have $\frac{\partial \tilde{v}_3}{\partial v_3}(p_3) = \frac{\phi_z^3(\mathbf{0})}{(\phi_x^1(\mathbf{0}))^2}$.

Then the above calculations give

$$\begin{aligned}\Phi_*^3(\ell) &= span\left\{\left(b\frac{\partial \tilde{u}_3}{\partial u_3}(p_3) + c\frac{\partial \tilde{u}_3}{\partial v_3}(p_3)\right)\frac{\partial}{\partial u_3} + \left(b\frac{\partial \tilde{v}_3}{\partial u_3}(p_3) + c\frac{\partial \tilde{v}_3}{\partial v_3}(p_3)\right)\frac{\partial}{\partial v_3}\right\} \\ &= span\left\{\left(b\frac{(\phi_y^2(\mathbf{0}))^2}{(\phi_x^1(\mathbf{0}))^3}\right)\frac{\partial}{\partial u_3} + c\frac{\phi_z^3(\mathbf{0})}{(\phi_x^1(\mathbf{0}))^2}\frac{\partial}{\partial v_3}\right\}\end{aligned}$$

for $\ell = span\{b\frac{\partial}{\partial u_3} + c\frac{\partial}{\partial v_3}\}$ with $b, c \in \mathbb{R}$ and $b \neq 0$.

## References


[1] V.I. Arnol'd, Simple singularities of curves, Tr. Mat. Inst. Steklova 226 (1999) 27–35.
[2] A.V. Bäcklund, Ueber Flächentransformationen, Math. Ann. 9 (3) (1875) 297–320.
[3] Robert L. Bryant, Lucas Hsu, Rigidity of integral curves of rank 2 distributions, Invent. Math. 114 (2) (1993) 435–461.
[4] Gil Bor, Richard Montgomery, $G_2$ and the rolling distribution, Enseign. Math. (2) 55 (1–2) (2009) 157–196.
[5] A. Campillo, J. Castellanos, Curve Singularities: An Algebraic and Geometric Approach, Actualités Math., Hermann, 2005.
[6] A. Castro, R. Montgomery, Spatial curve singularities and the monster/semple tower, Israel J. Mat. (2012) 1–47, http://dx.doi.org/10.1007/s11856-012-0031-2.
[7] S.V. Duzhin, B.D. Chebotarevsky, Transformation Groups for Beginners, Stud. Math. Libr., vol. 25, Amer. Math. Soc., Providence, RI, 2004. Translated and revised from the 1988 Russian original by Duzhin.
[8] J. Favard, Cours de géométrie différentielle locale. Cahiers scientifiques, Gauthier-Villars, 1957.
[9] Frédéric Jean, The car with $n$ trailers: characterisation of the singular configurations, ESAIM Control Optim. Calc. Var. 1 (1995/1996) 241–266 (electronic).
[10] S. Kobayashi, K. Nomizu, Foundations of Differential Geometry, Wiley Classics Lib., vol. 1, Wiley, 1996.
[11] A. Kumpera, C. Ruiz, Sur l'équivalence locale des systèmes de Pfaff en drapeau, in: Monge–Ampère Equations and Related Topics, Florence, 1980, Ist. Naz. Alta Mat. Francesco Severi, Rome, 1982, pp. 201–248.
[12] A. Kumpera, J.L. Rubin, Multi-flag systems and ordinary differential equations, Nagoya Math. J. 166 (2002) 1–27.
[13] Shun-Jie Li, Witold Respondek, The geometry, controllability, and flatness property of the n-bar system, Internat. J. Control 84 (5) (2011) 834–850.
[14] Piotr Mormul, Goursat distributions not strongly nilpotent in dimensions not exceeding seven, in: Alan Zinober, David Owens (Eds.), Nonlinear and Adaptive Control, in: Lecture Notes in Control and Inform. Sci., vol. 281, Springer, Berlin, Heidelberg, 2003, pp. 249–261.
[15] Piotr Mormul, Multi-dimensional Cartan prolongation and special $k$-flags, in: Geometric Singularity Theory, in: Banach Center Publ., vol. 65, Polish Acad. Sci., Warsaw, 2004, pp. 157–178.
[16] Piotr Mormul, Singularity classes of special 2-flags, SIGMA Symmetry Integrability Geom. Methods Appl. 5 (2009), x+22.
[17] Piotr Mormul, Fernand Pelletier, Special 2-Flags in Lengths not Exceeding Four: A Study in Strong Nilpotency of Distributions, 2010.
[18] Richard Montgomery, Michail Zhitomirskii, Geometric approach to Goursat flags, Ann. Inst. H. Poincaré Anal. Non Linéaire 18 (4) (2001) 459–493.
[19] Richard Montgomery, Michail Zhitomirskii, Points and curves in the Monster tower, Mem. Amer. Math. Soc. 203 (956) (2010), x+137.
[20] Peter J. Olver, Applications of Lie Groups to Differential Equations, second edition, Grad. Texts in Math., vol. 107, Springer-Verlag, New York, 1993.
[21] Fernand Pelletier, Configuration Spaces of a Kinematic System and Monster Tower of Special Multi-Flags, 2011.
[22] Kazuhiro Shibuya, Keizo Yamaguchi, Drapeau theorem for differential systems, Differential Geom. Appl. 27 (6) (2009) 793–808.
[23] C.T.C. Wall, Singular Points of Plane Curves, London Math. Soc. Stud. Texts, Cambridge University Press, 2004.
[24] Oscar Zariski, The Moduli Problem for Plane Branches, Univ. Lecture Ser., vol. 39, Amer. Math. Soc., Providence, RI, 2006. With an appendix by Bernard Teissier. Translated from the 1973 French original by Ben Lichtin.